A Novel Formulation for Steady and Decaying Turbulent Line Vortices

Georgios Dimitriou Panagiotakakos

A Thesis

In The Department

Of

Mechanical Engineering

Presented in Partial Fulfillment of the Requirements

for the Degree of Master of Applied Science (Mechanical Engineering)

at Concordia University

Montreal, Quebec, Canada

April 2017

Concordia University

School of Graduate Studies

Abstract

A Novel Formulation for Steady and Decaying Turbulent Line Vortices

by

Georgios Dimitriou Panagiotakakos

Abstract

Based on the *n*-family of laminar vortex formulation, a new generalized model applicable to the turbulent kind is presented. The self-similarity of the phenomenon allows, through the application of Vatistas and Aboelkassem (2006) simple variable transformation, to simulate its decay phase.

For the steady-state case, given the Vatistas et al. (1991) exponent *n*, the value of the turbulent intensity parameter (β), intrinsic in the azimuthal velocity formula, is found by fitting the analytical tangential velocity to various experimental profiles with different effective Reynolds numbers using the Least Square Error (LSE) method. Alike to the laminar *n*-family, $n = 2$ gives the smallest error and thus the best approximation. Also taking β to be constant or varying with the radius produces insignificant differences in the velocity profile. Thus, in order to close the system, the tangential velocity with $n = 2$ and a constant β that minimizes the error is inducted into the analysis. When β is plotted against the effective Reynolds number, a coherent relationship

amongst the two emerges. An empirical equation, which connects the two properties, is then constructed. This gives the ability to researchers to approximate the velocity (tangential, axial and radial components) using only three parameters: the effective Reynolds number, the core radius, and the maximum tangential velocity.

Application of the abovementioned variable transformation to the steady turbulent vortex yields its corresponding decaying version. The validity of the model is tested for several laminar and turbulent cases. The tangential velocity decay of fixed wing aircraft wake, and rotating helicopter blade tip turbulent vortices, approximated using the new model provides more realistic results than the traditional circulation approach. The profiles of the last property, that is routinely used in aviation to define the hazard threshold in order to provide a safe aircraft separation distance in large airports, is found to be lacking in representing the real cases of diminishing vortices. The previous lies on the fact that the assumed flattening of the circulation curve at large radii, applicable to laminar cases it is not true when the vortex is turbulent. Consequently, the prescribed value of the radius (e.g. 7 times the core radius) to represent the circulation at "infinity" proposed by Squire (1965) and Iversen (1976), implemented also in numerous other models like Burnham and Hallock (1982) and Proctor (2000), must be reconsidered. Future work should focus on the definition of the hazard threshold based on the tangential velocity instead of its circulation signature.

Acknowledgments

The completion of this thesis which marks the completion of my post graduate studies brings to an end an important and fascinating chapter of my life. At this point I have to express my deepest and sincere gratitude to the people that have contributed to this personal achievement. First and foremost I want to express my immeasurable appreciation and respect to my supervisor Dr George H Vatistas for his expert guidance, understanding, financial support, and encouragement throughout my postgraduate studies. Without his valuable advices the completion of this thesis won't be feasible. Moreover, I could not imagine having a more influential person and a greater mentor guiding me.

I would also like to express my deepest gratitude to my parents Dimitris and Katerina and my brother Christos for their unconditional love and trust that they show to every aspect in my personal and academic life.

Last but not least I would like to express my gratefulness to my relatives in Montreal and my best friend Christos for supporting me and emotionally encouraging me during those two years of my studies.

To all of them and especially to my parents I dedicate this thesis.

Thesis Title:
A Novel Formulation for Steady and Decaying Turbulent line Vortices

Table of Contents

List of figures

List of tables

Nomenclature

A	span times chord length	m^2
c	chord length	m
c_d	drag coefficient	dimensionless
r, z	Radial and axial coordinates	m
r_c	Core radius	m
V_r, V_θ, V_z	Radial, tangential and axial velocity components	m/s
$V_{\theta c}$	Maximum tangential velocity at the core	m/s
k	Lamb's constant	dimensionless
l	Mixing length	m
M	Rolling moment	N m
p	Static pressure	Pa
u	Dimensionless radial velocity component	dimensionless $\left(V_r / V_{\theta c}\right)$
w	Dimensionless axial velocity component	dimensionless $\left(V_z / V_{\theta c}, \zeta h\right)$
V	Normalized tangential velocity component	dimensionless $\left(V_\theta / V_{\theta c}\right)$
$\mathrm{Re_v}$	Vortex Reynolds number	dimensionless $\left(\rho V_{\theta c} r_c / \mu\right)$

Re_{veff}	Effective Vortex Reynolds number	dimensionless $\left(\rho V_{\theta c} r_c / \mu_{eff}\right)$
Ri	Richardson number	dimensionless
U	Normalized radial velocity component	dimensionless $\left(\beta \mathrm{Re}\, u\right)$
H	Normalized axial velocity component	dimensionless $\left(\beta \mathrm{Re}\, h\right)$
h	Axial velocity parameter	dimensionless (w/ζ)
m	Exponential constant	dimensionless
n	Index of the family of vortices	dimensionless
o	Order of magnitude	dimensionless
Δp	Static pressure change	Pa $\left(p - p_\infty\right)$
F_d	Drag force	N
f	Viscous dissipation function	dimensionless $\left(\xi^2 \left\{ \frac{d}{d\xi}\left(\frac{V}{\xi}\right)\right\}^2\right)$

Greek Letters

α	Squire's constant	dimensionless
α_I	Iversen's constant	dimensionless
α_L	Lambs constant	dimensionless
ν	Molecular kinematic viscosity	m^2 / s
ν_T	Turbulent kinematic viscosity	m^2 / s
ν_{eff}	Effective kinematic viscosity	m^2 / s
μ	Molecular viscosity	Kg / ms

μ_{eff}	Effective viscosity	Kg / ms
μ_T	Turbulent viscosity	Kg / ms
θ	Azimuthal coordinate	dimensionless
ρ	Density	Kg / m^3
ξ	Dimensionless radial coordinate	dimensionless $\left(r / r_c\right)$
ζ	Dimensionless axial coordinate	dimensionless $\left(z / r_c\right)$ (ζ, when appropriate could also represent the wake age, in radians)
β	Turbulent intensity parameter	dimensionless
$\overline{\beta}$	Parametrical Turbulent intensity parameter	dimensionless
η	Similarity variable	dimensionless
τ	Dimensionless time	$\left(1+4\nu t / r_c^2\right)$
τ'	Dimensionless time	$\left(4\nu t / r_c^2\right)$
Π	Dimensionless static pressure	$\left(p / \rho_\infty V_{\theta\max}^2\right)$
Γ_∞	Vortex circulation at large radius	m^2 / s
Γ_o	Initial Vortex circulation	m^2 / s
Γ	Vortex circulation	m^2 / s
σ	Standard deviation	dimensionless
Ω_z	Vorticity	rad/s $\left(\frac{1}{r}\frac{d}{r}\left(rV_\theta\right)\right)$

Operators used

∂	Partial derivative	dimensionless
$\frac{D}{Dt}$	Material derivative	1/s $\left(\frac{\partial}{\partial t}+V_r\frac{\partial}{\partial r}+\frac{V_\theta}{r}\frac{\partial}{\partial \theta}+V_z\frac{\partial}{\partial z}\right)$
∇^2	Laplacian	$1/m^2$ $\left(\frac{\partial^2}{\partial r^2}+\frac{1}{r}\frac{\partial}{\partial r}+\frac{1}{r^2}\frac{\partial^2}{\partial \theta^2}+\frac{\partial^2}{\partial z^2}\right)$

Subscripts

∞	Infinity
c	Vortex core
o	Properties on the vortex core

1. Introduction

The concept of a vortex in fluid mechanics can be defined as the region in a fluid in which the flow is rotating around a straight or curved axis. Rotational flows of this type are present in the majority of the natural phenomena as well as industrial machinery. Tornadoes, tropical cyclones (hurricanes and typhoons), volcanic, polar, and galactic vortices belong to the natural paradigms, where industrial applications include various elements of turbo-machinery, vortex separators, combustors, incinerators, heat exchangers, steam traps, diffusers and nozzles, plasma arcs, fluidic devices, vortex tubes, and wing tip vortices and many others.

During the takeoff or landing phases of the flight, the wake vortices generated by modern large civil aircraft poses serious control risks to the following airplane. As the demand for bigger and bigger aircrafts increase, studies aiming to find better ways to describe wing tip vortices have become a very active topic of research among many studies. An example is the wake vortex estimation of hazard control that defines the limiting time between two consecutive take offs and landings between aircrafts. The most widely used is AVOSS (Aircraft Vortex Spacing System) developed by NASA and adopted by nearly every traffic controller agency worldwide. The approach that this system uses is based on the dated pure laminar vortex model of Burnham and Hallock (1982), which along with the other parameters result to longer safety time frames than the essential. An improved model that will predict the time decay more accurately will be an innovation in aviation's *status quo*. The decay characteristics of the vortex, that can be a potential hazard, should be based on an advanced formulation that considers turbulent vortices unlike the laminar that are currently in use. Furthermore, a model that has the versatility to approximate laminar as well as vortices of different turbulence intensities can be beneficial to numerous

engineering applications. In the literature review section that follows, the most popular models both for laminar and turbulent cases will be briefly presented and their limitations will be identified.

1.2 Previous work

1.2.1 Laminar steady vortex formulations

The Rankine vortex model

Rankine (1858) was the first to translate the vortex motion characteristics into a mathematical equation. Rankine model related the tangential velocity profile to the radius dividing the vortex filament into two different areas: 1) rigid-body rotation inside the vortex core ($0 \le r \le r_c$) where the tangential velocity increases linearly, and 2) free-body rotation outside the vortex core $r \ge r_c$, where the tangential velocity reduces hyperbolically with the radius:

$$V \propto \begin{cases} \xi \ \ for \quad \xi < 1 \\ 1/\xi \ for \quad \xi \ge 1 \end{cases} \tag{1.1}$$

Rankine's model is the first that gave a scientific scope in the vortex motion kinematics but has several drawbacks that makes it an out-dated tool for use in today's research. The assumption that the radial and axial velocity components are zero in addition to the discontinuity that the vorticity $\left(\Omega_z\right)$ possesses at the core $r = r_c$ (Vatistas (1998)), weakens the physical validity of the model, let alone the substantial differences of the predicted tangential velocity values near the core in comparison to the experimental measurements. Despite these limitations of the formulation many modern studies do use the model to examine vortex dominated flows.

The Burgers vortex model

In order to improve Rankine's model by eliminating the sharp peak of the tangential velocity distribution near the core, Burgers (1948) derived a model that smoothened the profile, and as such correlated better the experimental measurements near the vortex core. For this model, the equation for the tangential velocity component is given by,

$$V = \frac{1}{\xi}\frac{1-\exp(-\kappa\xi^2)}{1-\exp(-\kappa)} \tag{1.2}$$

The constraint that requires the maximum value of V occurs at $\xi = 1$ gives the value of $\kappa = 1.2564$. The tangential velocity profile was a considerable improvement of Rankine's model but yet the radial velocity profile becomes unbounded in flow fields of infinite extent.

The Kaufmann-Scully vortex model

It was first Kaufmann (1962) that introduced this model. Later on Scully (1975) employed it to study harmonic air-loads in helicopter rotors. Since then many other investigators have used it extensively to investigate mainly tip-vortices and is known either as the Scully or better the Kaufmann-Scully model. The tangential velocity component for this model is given by,

$$V = \frac{2\,\xi}{1+\xi^2} \tag{1.3}$$

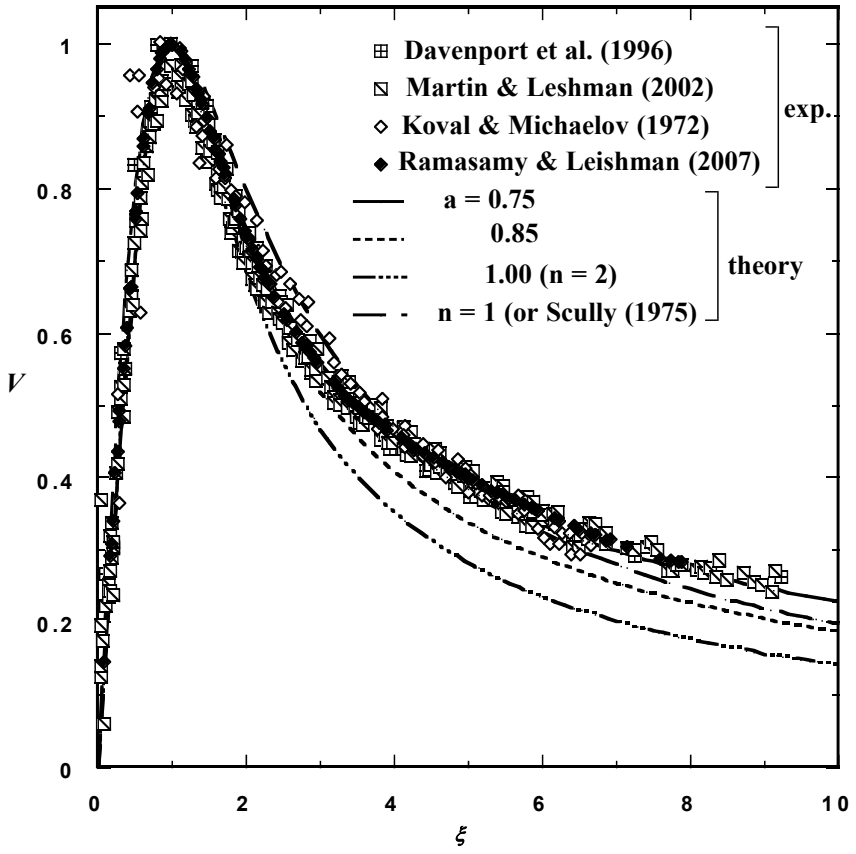

Figure 1.1: Tangential velocity profiles for vortices with varying degrees of turbulence intensity (a) Vatistas (2006). (Parameter a here is the reciprocal of β that will be used latter on in this thesis)

Vatistas (2006) showed that the normalized Scully's vortex approximated better turbulent tip vortices in the far field region ($\xi > \sim 3$) than the laminar formulations see Fig. 1.1. Based on the previous, he argued that this might explain the preferred choice by several past researchers.

The Vatistas vortex model

In 1991 Vatistas et al. proposed a new versatile model that can reproduce most of the previous popular models without their previously mentioned weaknesses. In this model the tangential velocity component is given by:

$$V = \frac{(2)^{\frac{1}{n}}\,\xi}{\left(1+\xi^{2n}\right)^{\frac{1}{n}}} \tag{1.4}$$

For different values of *n*, many of the classical models can be retrieved. Specifically, for $n = 1$ the Kaufmann-Scully model can be obtained. Furthermore for $n \to \infty$ the classical Rankines' model precipitates. Similarly, for *n* =2 the popular Lamb (1932)-Oseen (1912) or Burgers (1948) vortices can be closely approximated.

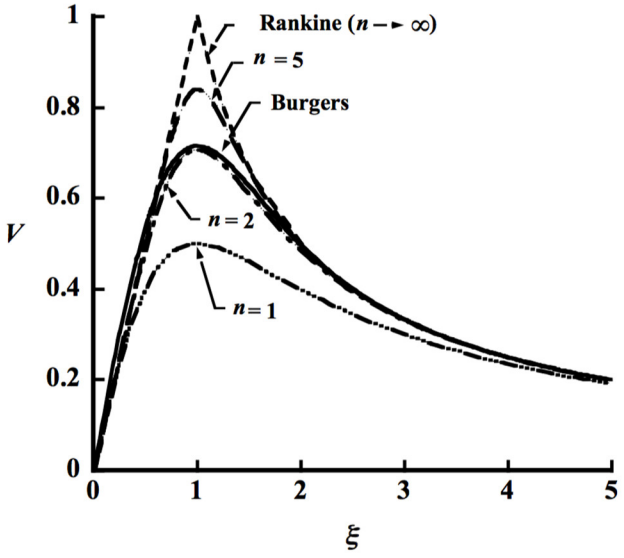

Figure 1.2. Distribution of tangential velocity component for the *n*-vortex profiles for various values of *n* (Credits: G.H.Vatistas)

1.2.2 Laminar decaying vortices

The Lamb-Oseen vortex model

The Lamb-Oseen model is an exact solution of the Navier-Stokes equations for one-dimensional axisymmetric vortex in polar coordinates where the turbulent (eddy) viscosity is assumed to be zero (fully laminar flow).

The differential (θ-momentum) equation for this time dependent flow field is given by,

$$\rho\left\{\frac{\partial V_\theta}{\partial t}\right\} = \mu_{eff}\left\{\frac{\partial^2 V_\theta}{\partial r^2} + \frac{1}{r}\frac{\partial V_\theta}{\partial r} - \frac{V_\theta}{r^2}\right\} \tag{1.5}$$

where ρ is the density of the fluid V_θ is the tangential velocity, t is the time, and r is the radial distance from the center of the axisymmetric vortex. The assumed initial ($t = 0$) velocity is that of a potential vortex,

$$V_\theta = \frac{\Gamma_o}{2\,\pi\, r} \tag{1.6}$$

Where Γ_o is the initial vortex circulation. The time evolution of the circulation is given by,

$$\Gamma(r, t) = \Gamma_o\left(1 - \exp\left[-\frac{r^2}{4\nu\, t}\right]\right) \tag{1.7}$$

where $\nu = \mu/\rho$ is the kinematic viscosity of the fluid. A qualitative time history of the circulation is shown in Fig. (1.3). Initially, the circulation (Γ_o) is constant for any radius possessing a jump

discontinuity at $r = 0$. As time proceeds the profile develops a depression near the axis of rotation gradually expanding outwards. As $t \to \infty, \Gamma(r) \to 0$.

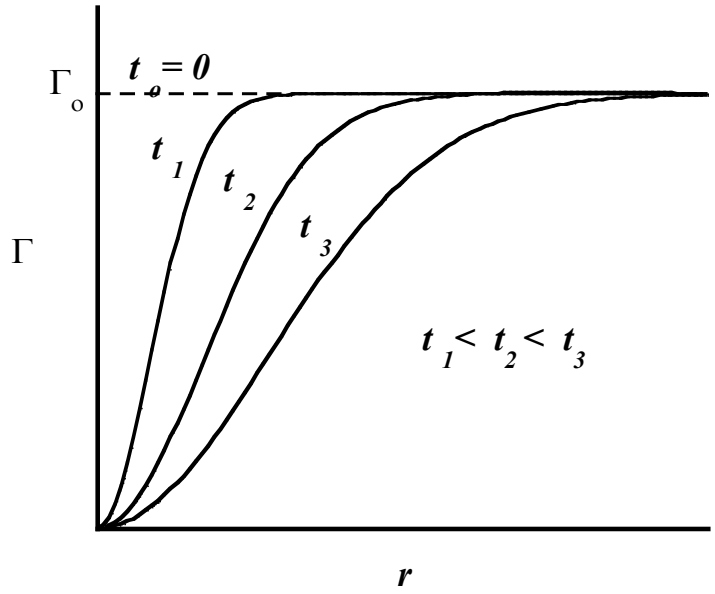

Figure 1.3. Circulation radial profiles for different time levels.

The radius of the maximum swirl velocity occurs at r_c. The last provides the value of Lambs constant α_L=1.25643. There is a debate for the origin of the decay mechanism formulation of the laminar vortex. Rossow (2006) states that Boltzmann (1894) suggested the transformation variable $\eta = r^2 / 4\,\nu\, t$, which reduces the partial differential equation into,

$$\rho\left\{\frac{\partial V_\theta}{\partial t}\right\} = \mu\left\{\frac{\partial}{\partial r}\frac{1}{r}\frac{\partial r\, V_\theta}{\partial r}\right\} \tag{1.8}$$

Using the similarity variable η, Eq. (1.8) can be easily integrated to yield the Lamb-Oseen velocity distribution:

$$V(\eta) = \frac{1}{\eta}\{1 - \exp(-\eta\}) \tag{1.9}$$

or

$$V(r,t) = \frac{\Gamma}{2\,\pi\, r}\left\{1 - \exp(-\frac{r^2}{4\,\nu\, t}\right\} \tag{1.10}$$

From Eq. (1.10) the vorticity (Ω_z) is then given by,

$$\Omega_z = \frac{1}{r}\frac{\partial\, r\, V_\theta}{\partial r} = \frac{\Gamma_o}{2\,\pi\,\nu\, t}\exp\left(-\frac{r^2}{4\,\nu\, t}\right) \tag{1.11}$$

Initially Ω_z is concentrated at the origin and it is singular $(\Omega_z \to \infty)$. As time evolves it diffuses outwards and decays see Fig. (1.4), reaching the limit $\Omega_z(r) \to 0$ as $t \to \infty$.

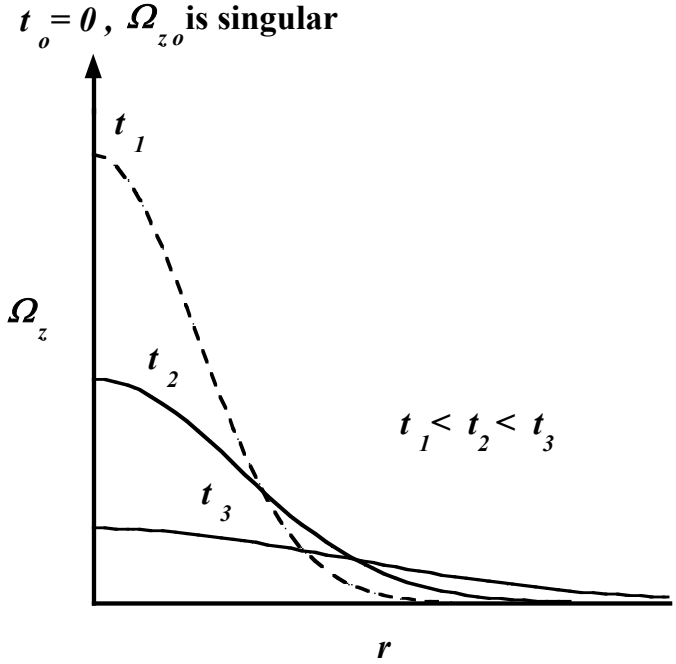

Figure 1.4. Vorticity radial profiles for different time levels.

The viscous core growth over time is given by,

$$r_c(t) = \sqrt{4 a_L \nu t} \tag{1.12}$$

The assumption of fully laminar flow leads to a viscous core growth prediction, which is considerably slower than the experimental results. In spite of the last, because of its simplicity, this model was used for years to model a diminishing aircraft wake vortex.

Other Laminar decaying laminar models

Other cases of decaying vortices could be obtained if one realizes that there is a space-time analogy associated with intense vortices if Boltzmann's (1894) η -variable is used as indicated by Vatistas and Aboelkassem, (2006). Based on this unique property, if a steady state solution is known, then the decaying form is obtained by a straightforward variable transformation. The process is also reversible, i.e. if the decaying solution is available, then the steady-state type can also be recuperated. Since the method does not require the initial velocity profile to be of the exponential function type, the transformation is more wide-ranging than Lundgren's (1982) method.

For example, consider Burger's vortex where the tangential velocity is given by:

$$V = \frac{1}{\xi}\frac{1-\exp(-\kappa\xi^2)}{1-\exp(-\kappa)} \tag{1.13}$$

Under the aforementioned transformation the above equation becomes:

$$V(\tau,\xi)=\frac{1}{\xi}\frac{\left(1-\exp\left[-\kappa\frac{\xi^2}{\tau}\right]\right)}{1-\exp[-\kappa]} \qquad \text{Where} \quad \tau=1+4\frac{\nu t}{r_c^2} \tag{1.14}$$

Similarly the tangential velocity of a decaying $n = 2$ vortex of Vatistas et al. (1991) yields,

$$V(\tau,\xi)=\frac{\sqrt{2}\,\xi}{\sqrt{\tau^2+\xi^4}} \tag{1.15}$$

1.2.3 Turbulent steady case

As presented above, there is a variety of models that were developed to analyze the laminar type of vortices yielding sufficiently acceptable predictions for most of the applications. However, the majority of cases in either nature or industry encounters with laminar flow phenomena are rare commodities since most of them involve turbulence. The complexity of the turbulent phenomena not only in the vortex field but also generally in Fluid Mechanics, is notorious. Historically, reasonable approximations to turbulent flows appeared much later than the laminar, almost near the second half of the 20th century. The main reason lies on fact that the collection of reliable measurements for turbulent vortices is very difficult, expensive, require sophisticated experimental procedures and techniques, and the evaluation and filtering of the extracted data depend heavily on many assumptions, resulting into several uncertainties, and often-debatable approaches. Furthermore, the diversity of the turbulent vortices that can manifest in different environments, combined with the limited experimental data makes the comparison of vortices with different levels of turbulence problematic. Nevertheless, fundamental contributions on this topic can be found in Newman (1959), Dosanjh et al. (1962) Hoffman and Joubert (1963), Squire [1965],

Iversen (1976), Tung et al. (1981), Ramasamy and Leishman (2007), and Vatistas (2006). In this part of the thesis only models that are intimately related to the present work will be discussed.

The Squire vortex model

Squire (1965) in order to include the turbulent effects extended the Lamb-Oseen laminar model to turbulent by incorporating an average turbulent "eddy" viscosity. Based on the hypothesis that the principal permanent characteristic of a line vortex is its circulation $\left(\Gamma_\infty\right)$ at a "large radius", where the total viscosity was considered to be the sum of the molecular plus the turbulent kinematic viscosity. The eddy viscosity was assumed to be a function of the circulation multiplied by a constant *a* (Squires constant*)*,

$$\nu_T = \nu + a\left(\frac{\Gamma_\infty}{2\pi}\right) \tag{1.16}$$

The averaged term of total viscosity $\left(\nu_{eff}\right)$ had to do with the fact that the value of eddy viscosity was assumed to be independent of the radial distance. This constant is numerically determined by matching $\left(\nu_{eff}\right)$ with the then available experimental data. The ratio of total to kinematic viscosity δ is then given by,

$$\delta = \frac{\nu_{eff}}{\nu} = 1 + \frac{\alpha}{2\pi}\left(\frac{\Gamma_\infty}{\nu}\right) = 1 + \alpha_L\left(\frac{\Gamma_\infty}{\nu}\right) \tag{1.17}$$

is used inside the viscous core ($0 < r < r_c$) growth prediction,

$$(\zeta) = \sqrt{4\alpha_L \delta\nu \left(\frac{\zeta}{\Omega}\right)} = \sqrt{\frac{4\alpha_L \delta\nu\zeta}{\Omega}} \tag{1.18}$$

This has been used as a comparable parameter of turbulence intensity to Reynolds number. Squire's contribution was the elimination of the singularity in Lamb-Oseen model for $t = 0$ as well as the establishment of the correlation of turbulent intensity to core growth over time. Furthermore, the development of a model, which relates the circulation at a large radius with the turbulent intensity, laid the foundations for the further development of the subsequent models of Iversen (1976) and Ramasamy and Leishman (2007).

The Iversen vortex Model

Based on Squires assumption that the principal permanent characteristic of a self-similar line vortex is its circulation at large radii, a function that correlated aircraft trailing vortex tangential velocity data in both on ground and flight experiments was introduced by Iversen (1976). Lamb's similarity variable produced the core growth expansion that is not in agreement with the new and improved experimental data. For this reason, Iversen modified the approach by introducing the mixing length hypothesis. It can be easily now understood that by replacing the viscosity parameter with the circulation at a large radius ($\mathrm{Re}_v = \Gamma_\infty / \nu$) in the similarity variable proposed by Lamb $\eta_l = -r^2 / 4\,\nu t$, η becomes now $-2\pi\eta_l / \Gamma_\infty$, and thus a more realistic model could be achieved.

Transforming the equation for the circulation,

$$\frac{\partial \Gamma}{\partial t} = r\frac{\partial}{\partial r}\left\{ \nu_{eff} r \frac{\partial}{\partial r}\left(\frac{\Gamma}{r^2}\right)\right\} + 2\nu_{eff} r \frac{\partial}{\partial r}\left(\frac{\Gamma}{r^2}\right) \tag{1.19}$$

in terms of the similarity variable η a new vortex model, which is parametrical to Reynolds number is obtained.

For the turbulent case, in order to satisfy the similarity relationship, Iversen incorporated the mixing length hypothesis $l = a_1 r$ into the total viscosity equation setting the eddy viscosity term to be proportional to the radius. In simple words Iversen gave the following equation for ν_{eff},

$$\nu_{eff} = \nu + l^2 r \frac{\partial}{\partial r}\left(\frac{\Gamma}{r^2}\right)$$

Where $l = a_1 r$ is the mixing length assumed to vary linearly with the radial distance across the vortex.

Thus the eddy viscosity term was formed based on Prandlt's mixing length concept for turbulent flows. However, this approach does not satisfy the actual physics, because it cannot resolve adequately the vortex transition region. For fully laminar flow ($\nu_T = 0$, $l = 0$) the equation of circulation collapses to Lamb-Oseen model as it should.

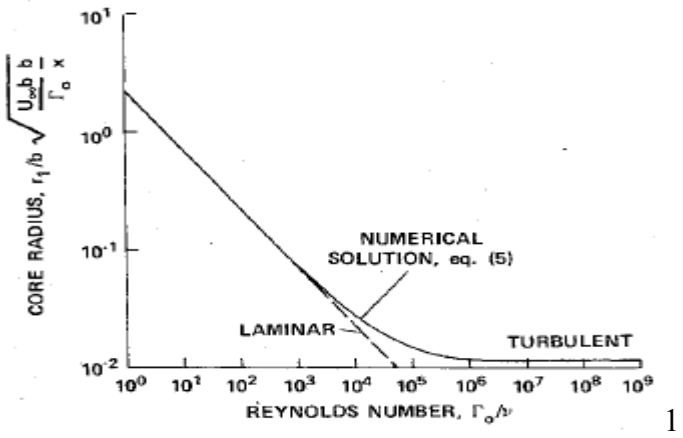

1

Figure 1.5. Core radius as a function of the vortex Reynolds number (Iversen (1976)). Note that $\Gamma_o \equiv \Gamma_\infty$.

The total viscosity variation proposed by Iversen came from analyzing the measurements of multiple Reynolds number vortices. He was able to obtain a value for $a_I = 0.01854$, which is now known as Iversen's constant.

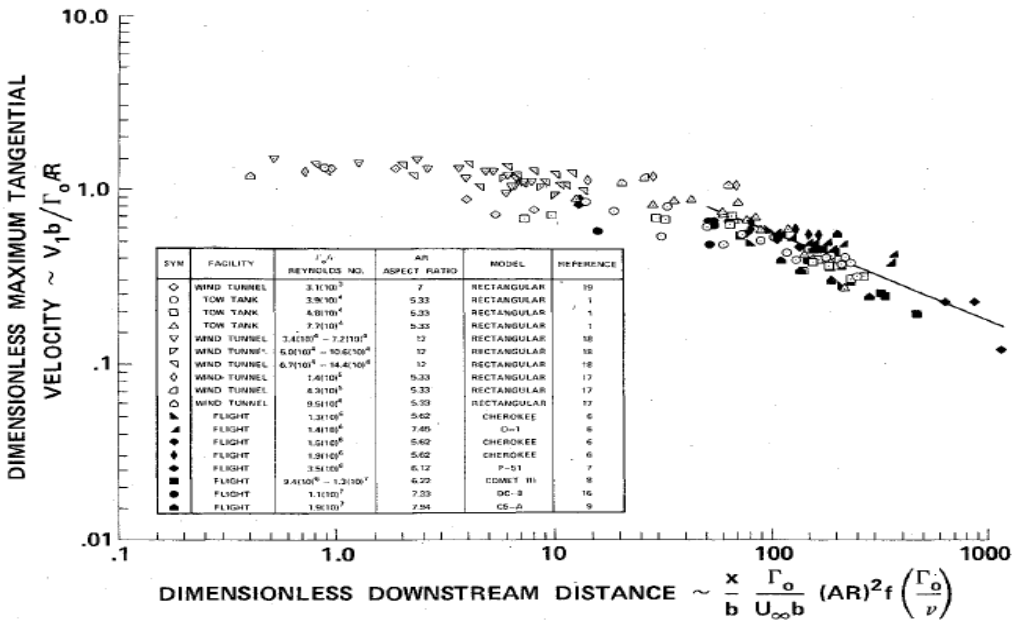

Figure 1.6. Maximum tangential velocity as a function of the downstream distance (Iversen (1976)). Note that $\Gamma_o \equiv \Gamma_\infty$.

The Ramasamy-Leishman vortex model

Ramasamy and Leishman (2007) in their paper on helicopter blade tip vortices, presented an updated model for turbulent tip vortices that examined the straining and diffusion of the viscous core of the turbulent vortices. Adopting Squires hypothesis that δ should be proportional to the circulation and following a similar transformation (as Iversen) they constructed an improved formulation that also included the effects of vortex wandering. Having access to precise measuring equipment obtained improved measurements they corrected Iversen's constant. Moreover using corrected Richardson number (Bradshaw (1969)),

$$R_i = \frac{2V_\theta}{r^2}\frac{d(rV_\theta)}{dr} \Big/ \left\{ r\frac{d\left(\frac{V_\theta}{r}\right)}{dr} \right\}^2 \qquad (1.21)$$

they provided a Vortex Intermittency function, which allows the multi-regional vortex theory to apply. Above the threshold of $Re_v^{1/4}$ the flow is laminar and any flow fluctuations will be dampened (the vortex will laminarize) and as the radial distance from the center of the core is increased the value of Richardson number progressively decreases below the threshold where turbulent effects appear. This weighting parameter was found to play an important role in modeling the vortex structure in a way that represented the real physics and allowed the model to collapse to Lambs model near the core of the vortex. The last improves on Iversen's approach in the outer regions where turbulence is present. The numerical solution used the 4th order Runge-Kutta to determine the numerous empirical constants. Finally, through the experimental observations it was confirmed that as the Reynolds number is increased, the turbulence of the flow increases, making the core growth rate to increase. This had an impact on the decay of the turbulent vortex as the peak swirl velocity reduces faster as the Reynolds number increases.

The Burnham-Hallock vortex model

In 1982 Burnham and Hallock presented a vortex model applied to turbulent vortices, which focused on the characteristics of the wake vortex that can create hazardous conditions in aircrafts. The proposed model for the tangential velocity profile is the same as the Kaufmann-Scully,

$$V_\theta = \frac{\Gamma_o}{2\pi}\frac{r}{r^2 + r_c^2} \qquad (1.22)$$

They selected a simple stochastic approach to transform the steady into a decaying vortex. The least squares stochastic procedure is not preferred over the simple stochastic procedure as it is supposed to be dependent on parameters such as the initial time t_o, and the standard deviation σ. Instead a probabilistic model, along with a wide variety of assumptions such as Gaussian distribution of the initial vortex strength with a standard deviation of 20% from the mean value of Γ_∞, fusing the previous two parameters into one $t_o = 3\sigma$ etc was proposed. The last is the basis for the decay stochastic process, and it is based on the assumption that vortices often decay in two stages: in the first stage the vortex strength remains constant and in the second it reduces rapidly.

The model was sufficient for the aviation needs back in 1982 however many of the assumptions made were rough. Although Burnham and Hallock (1982) attempted to reduce or even eliminate several empirical entries, the complexity of decaying turbulent flow still remained.

1.3 Contributions of the thesis

This thesis reports on a simple mathematical model applicable to steady and decaying turbulent vortices. The effectiveness of the model is verified by comparisons with various experimental observations especially with those with high turbulent intensity, and is found to be better to those in use today. A new equation that relates the turbulence intensity parameter to the effective Reynolds number is presented and discussed. An investigation on how a variable or simply constant intensity parameter influences the development of the dominant tangential velocity component shows not to be significantly different. Finally, the behaviour of diverse turbulent decaying vortices is illustrated. The circulation profiles that are currently in practice to

determine the hazards posed by wake aircraft vortices are examined and their validity is evaluated using the new approach.

2. Mathematical Formulation of the Problem

2.1 General Formulation of Incompressible Intense Vortices

The mathematical modeling of the problem requires that several assumptions should be made. For this reason a steady, incompressible, turbulent, and free of body forces, axisymmetric vortex is presupposed. The governing equations that will be used to mathematically represent the problem under consideration are the conservation of mass (continuity) and momentum equations (Navier-Stokes) in cylindrical coordinates (see Fig 2.1):

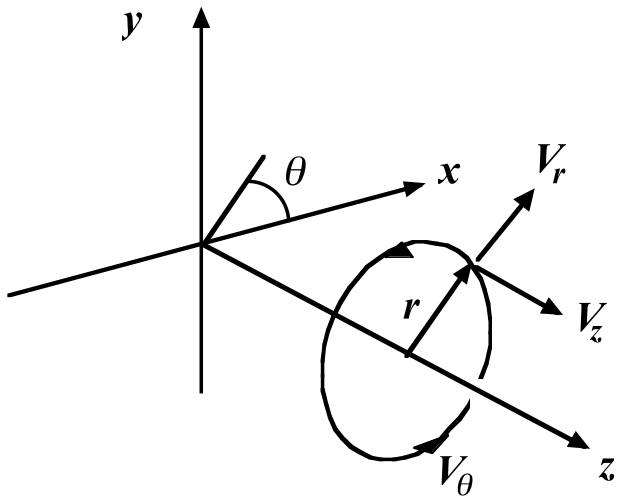

Figure 2.1. The coordinate system

Conservation of mass:

$$\frac{\partial V_r}{\partial r} + \frac{V_r}{r} + \frac{\partial V_z}{\partial z} = 0 \qquad (2.1)$$

Radial momentum:

$$\rho\left\{V_r\frac{\partial V_r}{\partial r}+V_z\frac{\partial V_r}{\partial z}-\frac{V_\theta^2}{r}\right\}=-\frac{\partial \Delta p}{\partial r}+\mu_{eff}\left\{\frac{\partial^2 V_r}{\partial r^2}+\frac{1}{r}\frac{\partial V_r}{\partial r}-\frac{V_r}{r^2}+\frac{\partial^2 V_r}{\partial z^2}\right\} \tag{2.2}$$

Axial momentum:

$$\rho\left\{V_r\frac{\partial V_z}{\partial r}+V_z\frac{\partial V_z}{\partial z}\right\}=-\frac{\partial \Delta p}{\partial z}+\mu_{eff}\left\{\frac{\partial^2 V_z}{\partial r^2}+\frac{1}{r}\frac{\partial V_z}{\partial r}+\frac{\partial^2 V_z}{\partial z^2}\right\} \tag{2.3}$$

Tangential momentum:

$$\rho\left\{V_r\frac{\partial V_\theta}{\partial r}+V_z\frac{\partial V_\theta}{\partial z}+\frac{V_r V_\theta}{r}\right\}=\mu_{eff}\left\{\frac{\partial}{\partial r}\frac{1}{r}\frac{\partial V_\theta}{\partial r}+\frac{\partial^2 V_\theta}{\partial z^2}\right\} \tag{2.4}$$

The contribution of turbulence is included here by means of an enhanced constant value for the effective viscosity, $\mu_{eff}=\mu+\mu_T$.

As we are dealing with strong (or intense) vortices it is customary to assume that the tangential velocity is dominant by several orders of magnitude as compared to the radial and axial components (see Table 1). Hence, the traditional assumption (Vatistas et al. (1991)) that the velocity vector has the form

$$\mathbf{q}(t,r)=\left[V_r(t,r),\, V_\theta(t,r),\, V_z(t,r)=z\,h_z(t,r)\right] \tag{2.5}$$

is implemented.

In order to generalize the results, the use of the flowing dimensionless parameters as suggested by Aboelkassem and Vatistas (2007) will be considered:

$$\xi = r / r_c$$

$$\zeta = z / r_c$$

$$u = V_r / V_{\theta c}$$

$$w = V_z / V_{\theta c} = \zeta h$$

$$V = V_\theta / V_{\theta c}$$

$$V_{\theta c} = \Gamma_\infty / 2\pi r_c$$

$$\Delta p = p - p_\infty$$

$$\Pi = \Delta p / \rho_\infty V^2{}_{\theta c}$$

$$Re = \rho_\infty V_{\theta c} r_c / \mu$$

$$\tau = \frac{v_{eff} t}{r_c{}^2}$$

where subscript "c" identifies properties at the vortex core (defined as the radius where the tangential velocity attains its maximum).

Recasting the governing equations in terms of the dimensionless groups, subject to condition given by Eq. (2.5) yields:

Continuity

$$\frac{\partial u}{\partial \xi} + \frac{u}{\xi} + h = 0 \qquad (2.6)$$
$$\delta \quad \delta \quad \delta$$

Table 2.1. Typical values of the vortex Reynolds numbers (Vatistas (1998))

Type of vortex	r_c (m)	$V_{\theta\,\max}$ (m/s)	Re	δ
Tornadoes	10.0	60.0	4.0 10^7	o (10^{-7})
Dust devils	3.0	10.0	5.0 10^6	o (10^{-6})
Whirl pools	15.0	5.0	7.5 10^7	o (10^{-7})
Cyclone chamber and wing tip vortices	0.2	0.5	6.7 10^5	o (10^{-5})
Bath tub vortices	0.2	0.1	2.0 10^4	o (10^{-4})
Aerodynamic	1.0	10.0	6.7 10^5	o (10^{-5})

r-momentum

$$\mathrm{Re}_{veff}\left\{u\frac{\partial u}{\partial \xi}-\frac{V^2}{\xi}\right\}=-\mathrm{Re}_{veff}\frac{\partial \Pi}{\partial \xi}+\frac{\partial^2 u}{\partial \xi^2}+\frac{1}{\xi}\frac{\partial u}{\partial \xi}-\frac{u}{\xi^2} \tag{2.7}$$

$1/\delta\ (\delta\,\delta \quad 1) \quad (1/\delta)\,\delta \quad \delta \quad \delta \quad \delta$

z-momentum

$$\mathrm{Re}_{veff}\left\{u\frac{\partial h}{\partial \xi}+h^2\right\}=-\frac{\mathrm{Re}}{\xi}\frac{\partial \Pi}{\partial \zeta}+\frac{\partial^2 h}{\partial \xi^2}+\frac{1}{\xi}\frac{\partial h}{\partial \xi} \tag{2.8}$$

$1/\delta\ (\delta\,\delta \quad \delta^2) \quad (1/\delta)\,\delta \quad \delta \quad \delta$

θ-momentum

$$\mathrm{Re}_{veff}\left\{u\frac{\partial V}{\partial \xi}+\frac{Vu}{\xi}\right\}=\frac{\partial^2 V}{\partial \xi^2}+\frac{1}{\xi}\frac{\partial V}{\partial \xi}-\frac{V}{\xi^2} \tag{2.9}$$

$1/\delta\ (\delta\,1 \quad 1\delta) \quad 1 \quad 1 \quad 1$

Neglecting the terms with order of magnitude δ or smaller, the above equations are reduced into:

Continuity:

$$\frac{\partial u}{\partial \xi}+\frac{u}{\xi}+h=0 \tag{2.10}$$

r- momentum:

$$\frac{V^2}{\xi}=\frac{d\Pi}{d\xi} \tag{2.11}$$

z - momentum:

$$\frac{d\Pi}{d\zeta}=0 \tag{2.12}$$

θ-momentum

$$\frac{u}{\xi}\frac{d(\xi V)}{d\xi}=\frac{1}{\mathrm{Re}\, v_{eff}}\frac{d}{d\xi}\left\{\frac{1}{\xi}\frac{d(\xi V)}{d\xi}\right\} \tag{2.13}$$

For the proper conversion of the physical problem into mathematics, in addition to the field equations, appropriate boundaries conditions are required. These are:

(i) $\xi = 0$, $V = u = 0$ and $\frac{\partial h}{\partial \xi} = 0$

(ii) $\xi \to \infty$, $V \to 0$

The system represented by Eqs. (2.10), (2.11), and (2.13) is underdetermined. Note that Eq. (2.12) indicates only that the pressure is not a function of the axial coordinate. As in the laminar case (Vatistas et al. (1991)), in order to close the system a realistic tangential velocity profile is considered by induction and then the rest of fluid parameters are obtained by deduction.

2.2 A Generalized Tangential Velocity Profile

Vatistas et al. (2015) proposed a model that approximates reasonably well the turbulent effects. As mentioned before, the induction of a tangential velocity equation will close the system. The simple algebraic equation for the radial profile of the tangential velocity that will accomplish the task is:

$$V(\xi) = \xi \left\{ \frac{1+\beta}{1+\beta\xi^{2n}} \right\}^{m} \tag{2.14}$$

Where β is the turbulent intensity parameter and $m = (1+\beta)/2n\beta$. If $\beta = 1$ we obtain,

$$V(\xi) = \xi \left\{ \frac{2}{1+\xi^{2n}} \right\}^{\frac{1}{n}}$$

This is the tangential velocity profile for the laminar *n*-family of vortices that was published in 1991 by Vatistas et al. (1991), and has been used by many researchers to study a variety of vortex dominated flows, see for example Tao et al. (2013), Antonini et al. (2015), Zheng et al. (2007), Brix et al. (2000), Murphy and MacManus (2011), Kecskemety and McNamara (2011), Ansari et al. (2006), and Ramesh et al. (2015). As it was remark in the introduction, with the proper choice of *n*, the classical models such as for example Rankine's ($n \to \infty$) and Kaufmann-Scully ($n = 1$) can be obtained. Letting $n = 2$ Burgers distribution could also be closely approximated. Different values of β will produce vortices with various degrees of turbulence i.e. for $\beta = 1$ laminar flow and when $\beta > 1$ simulates the turbulent kind with increasing intensity. The choice of the specific tangential profile equation will be based on how the Eq. (2.14) approximates the available experimental measurements.

The procedure of defining the value of the turbulent intensity β proceeds as follows. The square error is given by,

$$E = \sum_{i=1}^{n} \left\{ V_i - \xi_i \left(\frac{1+\beta}{1+\xi_{ii}^{2n}} \right)^{\frac{1+\beta}{2n\beta}} \right\}^2 \tag{2.15}$$

Given *n*, the value of parameter β that will minimize the square error is found solving the equation,

$$\frac{\partial E}{\partial \beta} = \frac{\partial}{\partial \beta} \sum_{i=1}^{n} \left\{ V_i - \xi_i \left(\frac{1+\beta}{1+\beta\xi_i^{2n}} \right)^{\frac{1+\beta}{2n\beta}} \right\}^2 = 0 \tag{2.16}$$

Otherwise, what is the value of n that will make the tangential velocity to pass through the discrete experimental data points (V_i, ξ_i) with the LSE. The procedure in finding which n will produce the least error is given next.

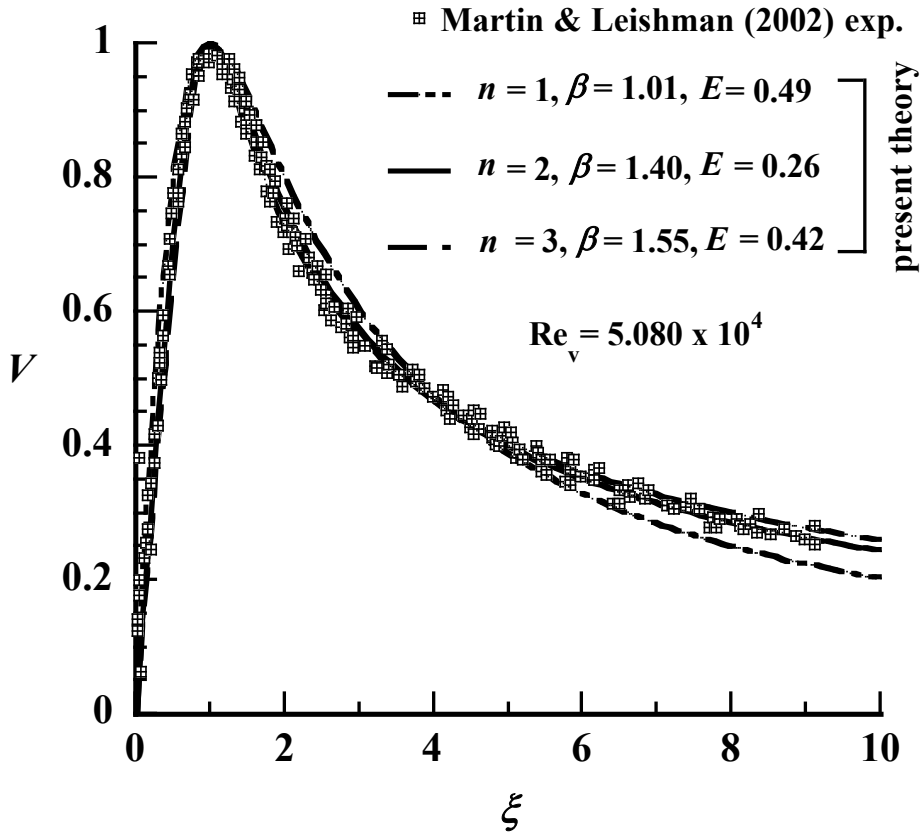

Figure 2.2. Square error E for different assumed tangential velocity profiles.

A value of n (say one) is selected. The root of Eq. (2.16) is then solved for β and the error E is recorded. The process is repeated with n = 2 and 3. As was also the case with the laminar n-family of vortices, n = 2 produces the best approximation for turbulent vortices, see Fig. 2.2).

Therefore, the equation for the tangential velocity distribution that will be used for the further developments will be takes the form,

$$V = \xi\left(\frac{1+\beta}{1+\beta\xi^4}\right)^m \tag{2.18}$$

Then the radial and axial velocity profiles can be determined from Eqs. (2.13) and (2.10) respectively,

$$u = \frac{\frac{\xi}{\mathrm{Re}_{veff}}\frac{d}{d\xi}\left\{\frac{1}{\xi}\frac{d}{d\xi}(\xi V)\right\}}{\frac{d(\xi V)}{d\xi}} \tag{2.19}$$

and

$$h = \frac{1}{\xi}\frac{\partial(\xi u)}{\partial \xi} \tag{2.20}$$

There is one more issue that has to be examined before the tangential velocity profile is inducted into the global formulation. Experimental evidence by Bhagwat and Leishman (2000) and Hoffman and Joubert (1963) revealed a multiregional vortex structure where the core is laminar near the axis of rotation (Fig. 2.3) region (1), followed by a region where the vortex is in a state of transition (2), maturing finally into a fully turbulent flow for larger radii (3). Martin and Leishman (2002) confirmed Squire's hypothesis that the effective viscosity increases with the radius using Laser Doppler Velocimetry (LDV). The assumption of multi-region vortex structure was based on the vortex Reynolds number, which argues that turbulence increases the rate of diffusion of vorticity caused by the straining effects in the laminar vortex core. Due to the last and depending on the Reynolds number, the viscous core expands over time at a certain rate, which later on gives rise to turbulence. There is ample experimental evidence that justifies the assertion that re-laminarization taking place near the core prevents any turbulent effects to appear.

Bradshaw(1969) as well as Holzapfel et al. (2001), introduced Richardson's number (ratio of potential to kinetic energy) to describe the local strength of stratification. Richardson's critical number, given as a function of Reynolds number was empirically determined by Cotel and Breidenthal (1999). Above $Re_v^{1/4}$ because of re-laminarization, turbulent flow fluctuations are damped see Fig. 3.4.

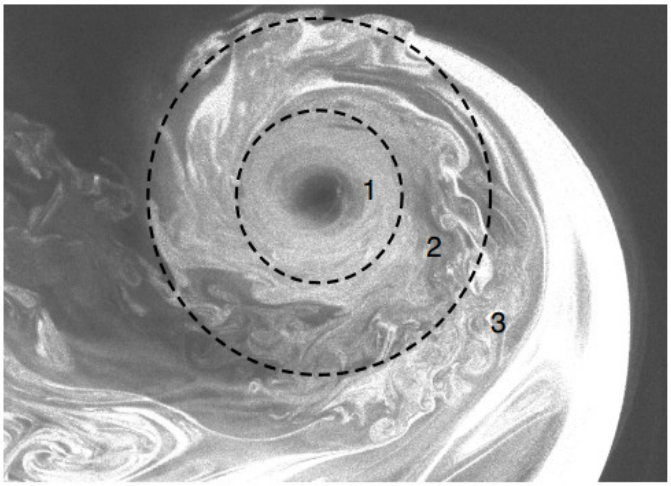

Region 1: Fully laminar
Region 2: Transitional
Region 3: Fully turbulent

Figure 2.3. Multiregional vortex structure (Ramasamy and Leishman (2007))

As illustrated in Figs. (2.2) and (2.3), the vortex core is completely laminar, and when the stratification threshold is crossed, turbulence starts to build up. There are several models that do not consider this variation assuming constant viscosity across the vortex filament. These predictions according to Ramasamy and Leishman (2007) are contentious.

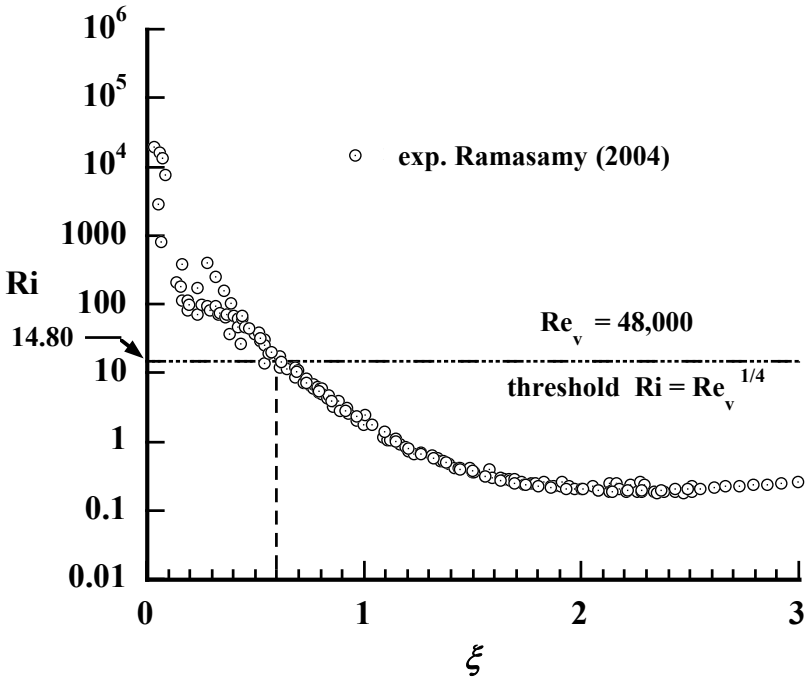

Figure 2.4. Variation of Richardson number for various models with non-dimensional Radial distance, $Re_v = 48{,}000$. (Adapted from Ramasamy and Leishman (2007)

In order to have a more general model where the vortex in the core is laminar and the turbulent intensity parameter $\bar{\beta}$ is one and progressively reaches the final value β where turbulent effects are fully developed, a function that relates $\bar{\beta}$ with ξ could be,

$$\bar{\beta}(\xi) = 1 + \left\{ \frac{1}{1+10^{(2.2-\xi)1.396}} - \frac{1}{1179.1} \right\} (\beta - 1) \tag{2.21}$$

In this case the value of β can be now obtained using the LSE method,

$$\frac{\partial E}{\partial \beta} = \frac{\partial}{\partial \beta} \sum_{i=1}^{n} \left\{ V_i - \xi_i \left(\frac{1+\bar{\beta}}{1+\bar{\beta}\,\xi_i^4} \right)^{\frac{1+\bar{\beta}}{4\bar{\beta}}} \right\}^2 = 0 \tag{2.22}$$

The radial profile of Eq. (2.21) with β = 1.38 is shown in Fig. (2.5). Near the axis of rotation the value of $\overline{\beta}$ is near 1, which implies a laminar vortex. At approximately ξ = 3, where turbulence is fully developed, $\overline{\beta}$ has reached 98% of its final value of 1.38. In the transition region, between $\xi \sim 0.6$ and 3), $\overline{\beta}$ varies from 1 to 1.35.

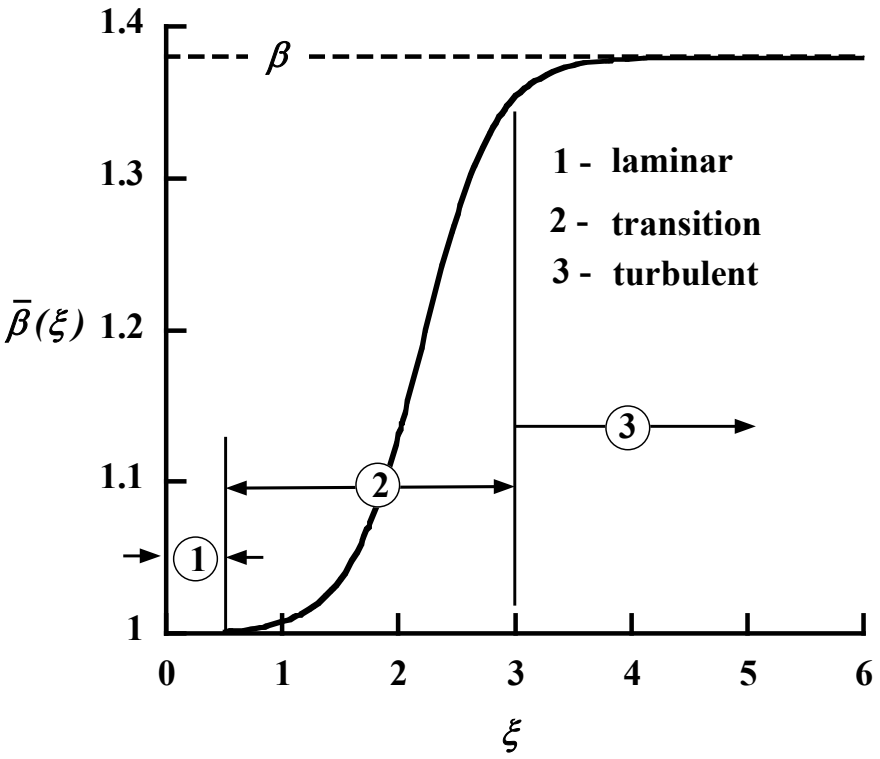

Figure 2.5. Variation of turbulence intensity parameter $\overline{\beta}$ with the dimensionless radius ξ, for β = 1.38.

In Fig. (2.6) the theoretical tangential velocity component, as a function of the radial distance along with the experimental data for constant β and variable $\overline{\beta}$, for three different datasets is depicted. It is amply evident that the velocity distributions do not differ significantly

for constant and variable values of β. The last could justify the use of the same value for beta across the vortex.

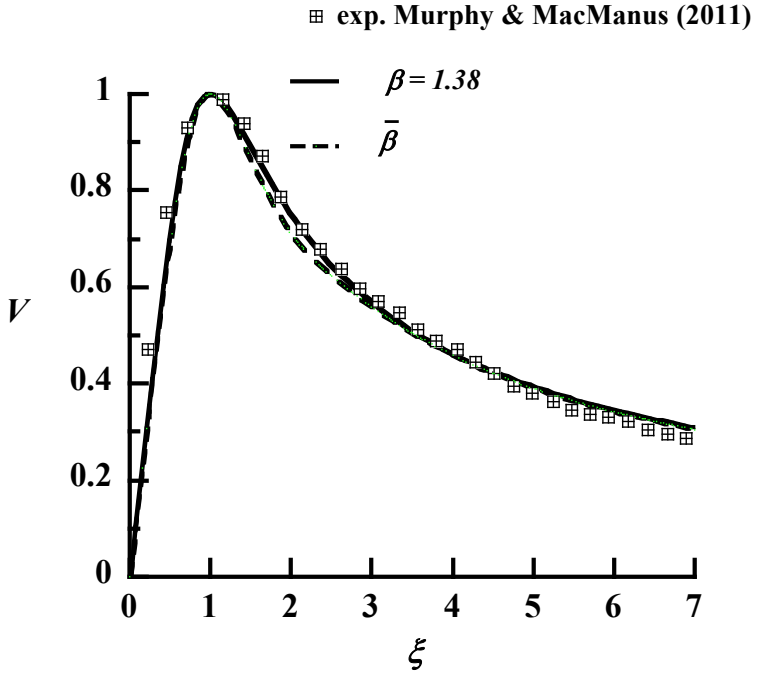

(a)

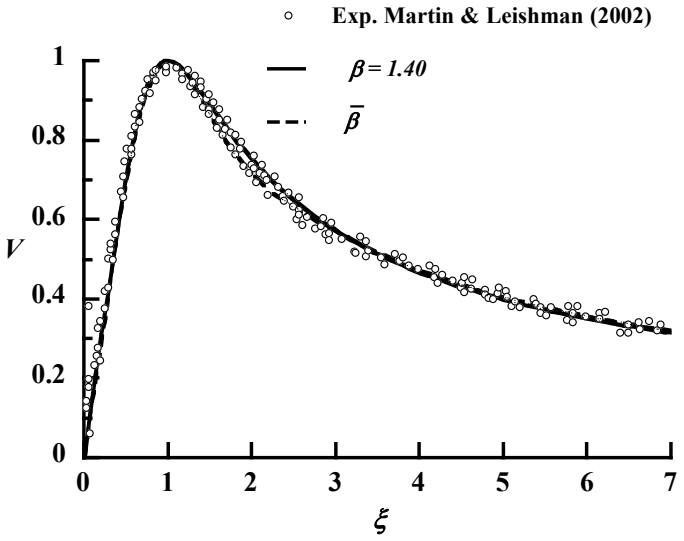

(b)

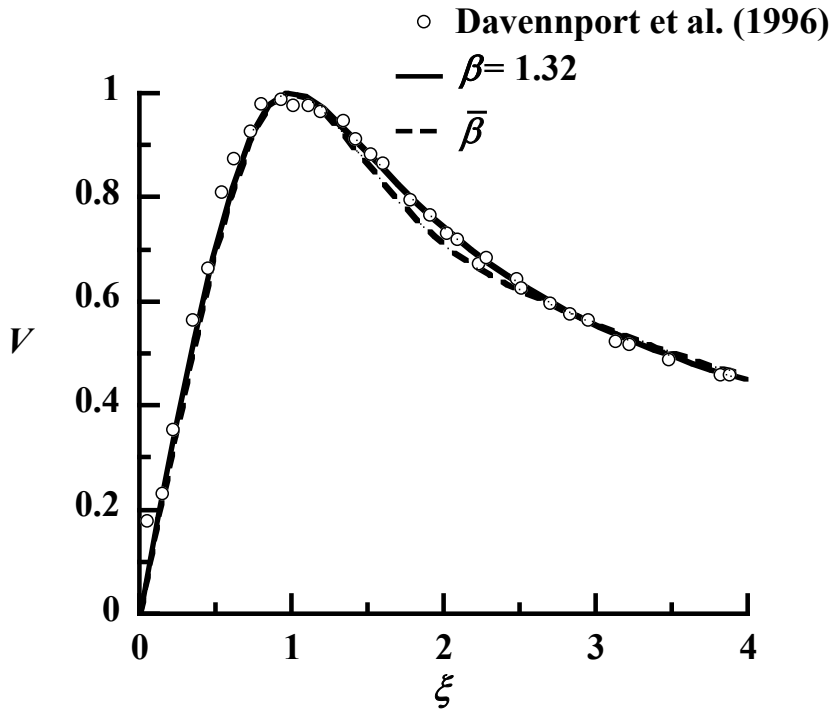

(c)

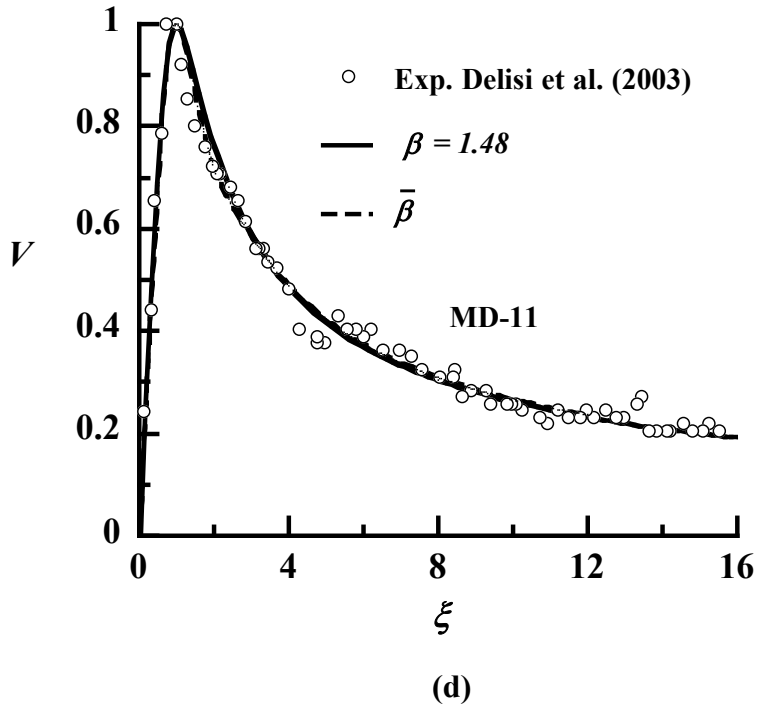

(d)

Figure 2.6. Velocity versus radial distance for three laboratory vortices (a), (b) & (c), and a full-scale vortex (d).

2.3 General Formulation of Decaying Vortices

The solutions that applied to the decay process belong to a particular class in which the velocity vector has the general form

$$\bar{\mathbf{q}}(\tau, \xi) = \left[u(\tau, \xi), V(\tau, \xi), w(\tau, \xi) = \zeta h(\tau, \xi) \right]$$

Following the same procedure as before, and using the simplified continuity and Navier-Stokes equations, the tangential-momentum equation is given by:

$$\frac{\partial V}{\partial \tau'} + u(\tau', \xi)\left(\frac{\partial V}{\partial \xi} + \frac{V}{\xi}\right) = \left\{\frac{\partial^2 V}{\partial \xi^2} + \frac{1}{\xi}\frac{\partial V}{\partial \xi} - \frac{V}{\xi^2}\right\} \tag{2.23}$$

Continuity:

$$\frac{\partial}{\partial R} u(\tau, \xi) + \frac{u(\tau, \xi)}{\xi} + h(\tau, \xi) = 0 \tag{2.24}$$

Radial momentum

$$\frac{[V(\tau, \xi)]^2}{\xi} = \frac{\partial \Delta p(\tau, \xi)}{\partial \xi} \tag{2.25}$$

Similar to laminar vortices, the time dependent tangential velocity of a turbulent vortex possesses a distinct self-similarity. When the velocity profiles at different time levels are normalized by their maximum values and are plotted against the dimensionless radius $(\eta = r / r_{\max})$ all profiles collapse into one, see Fig. (2.7) (a) for laminar, and (b) for turbulent (Fig. 36 in Martin and Leishman (2002)) vortices.

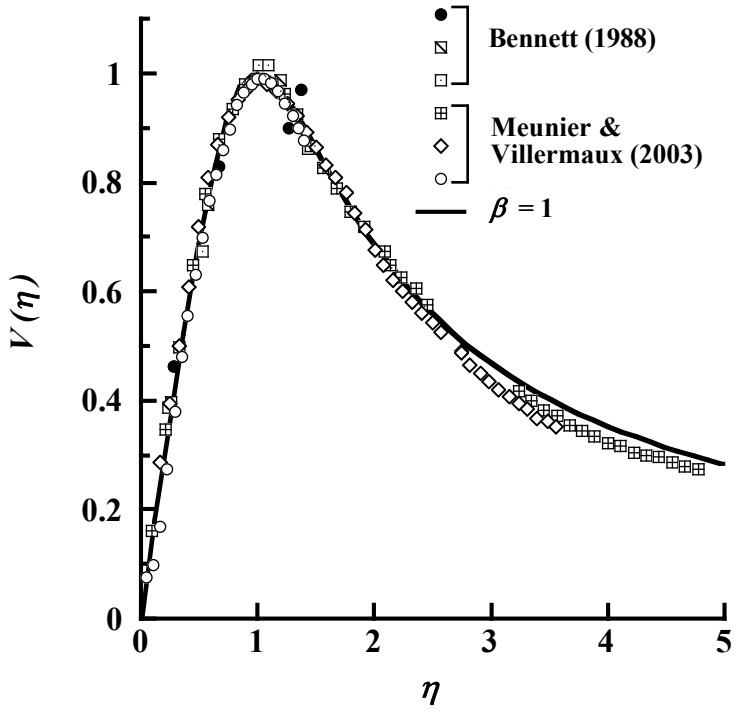

(a)

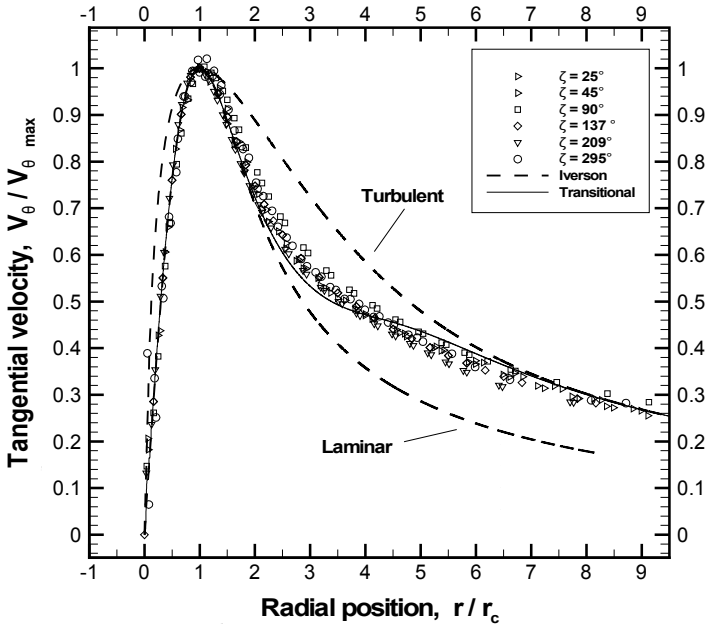

(b)

Figure 2.7 Collapse of the (a) laminar and (b) turbulent tangential velocity distributions in different time levels into one. The turbulent case was taken from Martin and Leishman (2002).

Using the dimensionless variable for time,

$$\tau = 1 + 4\frac{\nu t}{r_c^2}, \quad \tau = 1 + \tau', \quad \tau' = 4\frac{\nu t}{r_c^2} \tag{2.27}$$

and the following variable transformations as proposed by Vatistas and Adboelkassem (2006)

$$\begin{aligned} &\eta = \xi / \sqrt{\tau} && \text{(a)} && V(\tau, \xi)\sqrt{\tau} = V(\eta) && \text{(b)} \\ &U(\eta) = u(\tau, \xi)\sqrt{\tau} - 2\eta && \text{(c)} && \Delta\Pi(\eta) = p(\tau, \xi)\,\tau && \text{(d)} \\ &H(\eta) = h(\tau, R)\,\tau && \text{(e)} \end{aligned} \tag{2.28}$$

the governing equations can be transformed into the ordinary set:

$$\frac{U(\eta)}{\eta}\frac{d}{d\eta}\left(\eta g(\eta)\right) = \frac{d}{d\eta}\left(\frac{1}{\eta}\frac{d}{d}\left(\eta\, g(\eta)\right)\right) \tag{2.29}$$

Using continuity, we get

$$H(\eta) = -\frac{1}{\eta}\frac{d}{d\eta}\left[\eta\, U(\eta)\right] \quad \text{where} \quad H(\eta) = h(\tau, R)\,\tau \tag{2.30}$$

And from the radial-momentum

r-momentum

$$\frac{\left[g(\eta)\right]^2}{\eta} = \frac{d}{d\eta}\left(\Delta\Pi(\eta)\right) \tag{2.31}$$

These are analogous to the ones that have produced several steady solutions. For more details, please consult Vatistas and Adboelkassem (2006) or in the Appendix B.

This method will be used in the next section (Discussions of Results) to transform the steady turbulent into decaying vortex.

3. Discussions of Results

In the previous section, a new steady state vortex model, which also included the effects of turbulence were presented. Using the transformation of Vatistas and Aboelkassem (2006) the time decaying version was also outlined. In this chapter the validity of the results will be examined via comparisons to the already existing models and experimental evidence. Then the outcomes of the novel vortex approach will be critically discussed. Finally, the dangerous conditions posed by aircraft wake vortices will be assessed.

3.1. Steady turbulent vortices

Due to theoretical simplicity along with the large quantity of experimental measurements associated with laminar vortices, swirls of this kind are adequately covered by a variety of existing models such as for example Rankine (1858), Burgers (1948), Sullivan (1959), Vatistas et al. (1991) and several others. In contrast to the previous, the limitations of the measuring techniques and turbulence modeling prevented a theoretical formulation capable in describing the turbulent vortex as adequately as the laminar type.

Thus far we have designated the degree of turbulence with parameter β without providing its link to any of the flow properties. At the present it is imperative to make the required connection. The variation of parameter β with the vortex Reynolds number for both laboratory and large-scale vortices is given in Fig. 3.1. No obvious relation between β and the vortex Reynolds number (Re_v) among these vortices can be detected.

However, when β is plotted as a function of the effective Reynolds number $\left(\mathrm{Re}_{v\,eff}\right)$, using the total viscosity $\left(\nu_{eff}\right)$ relationship of Ramasamy and Leishman (2007),

$$\nu_{eff} = \left(1 + 6.5 \times 10^{-5}\ \mathrm{Re}_{v}\right) \nu \tag{3.1}$$

then the coherent correlation shown in Fig. (3.2) emerges.

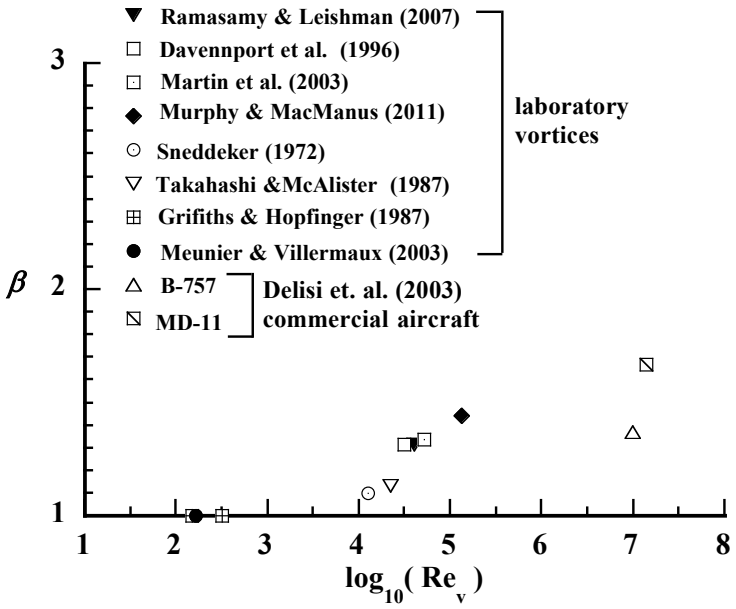

Figure 3.1. Variation of β with Rev for different vortices (Vatistas et al. (2015))

In an attempt to also provide a mathematical relationship between β and the effective Reynolds the subsequent empirical formula was constructed,

$$\beta = -\frac{2.5}{1 + \exp\left\{\dfrac{\log_{10}\left(\mathrm{Re}_{v\,eff}\right) - 4.35}{0.12}\right\}} + 3.5 \tag{3.2}$$

Eq. (3.2) along with the experimental data of a multitude of vortices is shown in Fig. (3.2).

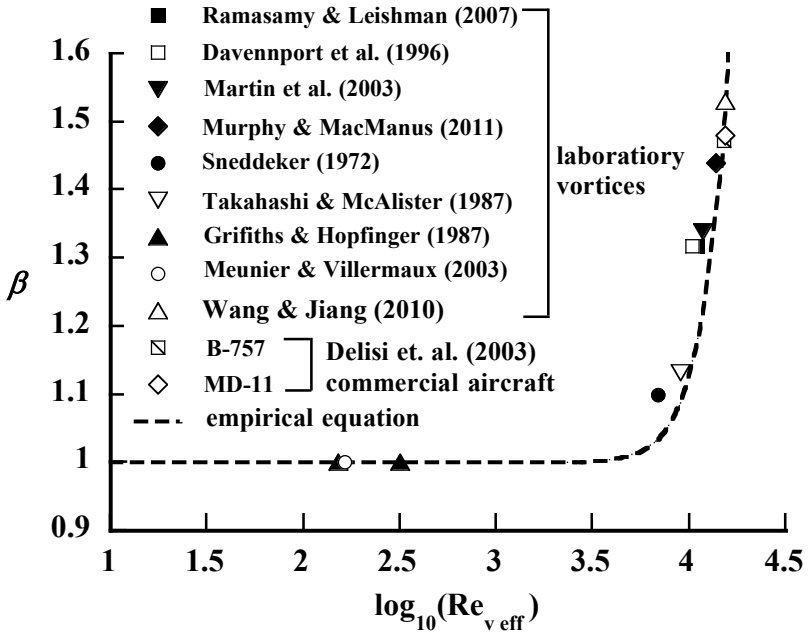

Figure 3.2. Variation of β with $Re_{v\,eff,}$ for different cases (enhanced version of Vatistas et al. (2015). The empirical equation refers to Eq. (3.1).

Enhanced viscosity models like Iversen's (1976) and Squire's (1965) although they correlate tolerably the observations, they do not then again predict the observed lift-up of the tangential velocity curve in the outer (free-vortex) region. As is illustrated in Fig. (3.3), the previous mentioned characteristic is clearly innate in the present model, whereby the tangential velocity is seen to lift-up and flatten, as it should be, with increasing β. Thus the new formulation provides a more realistic description of turbulent vortices.

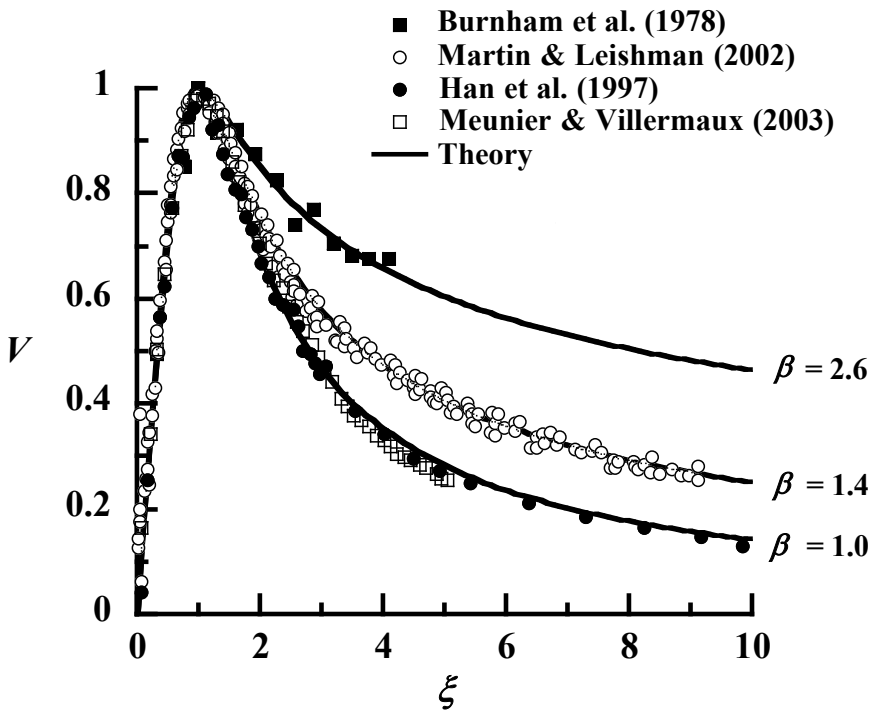

Figure 3.3. Lifting of the tangential velocity profile as turbulence parameter β increases.The theory here refers to Eq. (2.18).

Theoretical tangential velocity profiles together with the associated observed values for four vortices with different degrees of turbulence were given in Fig. 2.7. These, along with the four vortices provided in Fig. (3.3), and the additional profile shown in Fig. (3.4) are seen to approximate reasonably the actual experimental data. It is also self-evident; from Fig. (3.4) that Eq. (2.18) provides an improved approximation to turbulent vortices.

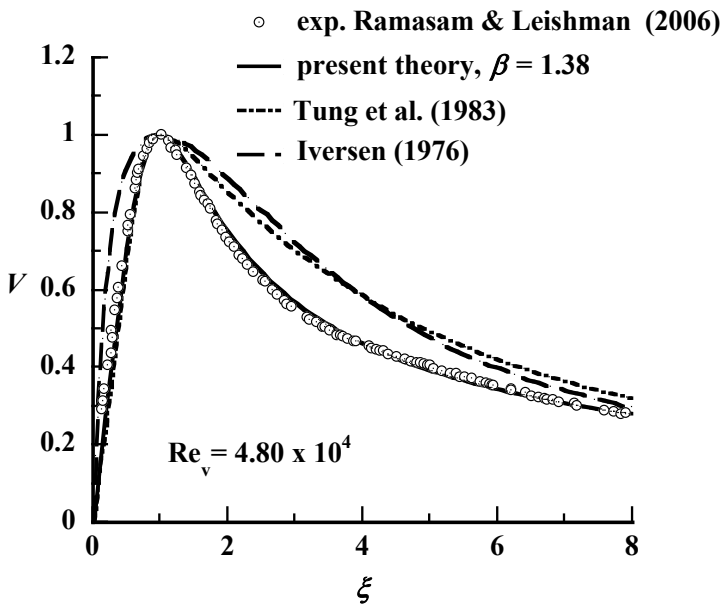

Figure 3.4 Tangential velocity profiles for medium turbulent intensity (β=1.38). Present theory here refers to Eq. (2.18).

Vortices shed by large commercial aircraft during takeoff and landing present a well-recognized danger to a smaller following plane, Holforty (2003). In the past, the vortex models of Rankine (1858), Hallock–Burnham (1978) (or Kaufmann (1962)–Scully (1975)), Lamb (1932)–Oseen (1912) (or Burgers (1948), and Hoffman–Joubert (1963) were used in determining the spacing limitation for commercial aircraft (Hinton and Tatnall (1997)). It is clear from Figs. (3.5), (3.6) and (3.7) that Eq. (2.18) provides a better approximation to the wake, than the traditional approaches for the vortices shed by a Boeing B-747, a McDonnell Douglas MD-11 wide-body and Boeing B-757 narrow-body aircrafts.

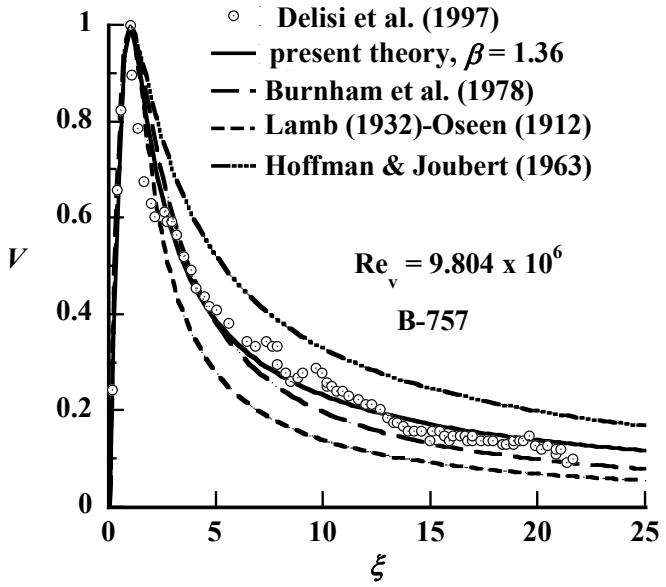

Figure 3.5 Tangential velocity profiles for different vortex models for a B-757. Present theory here refers to Eq. (2.18).

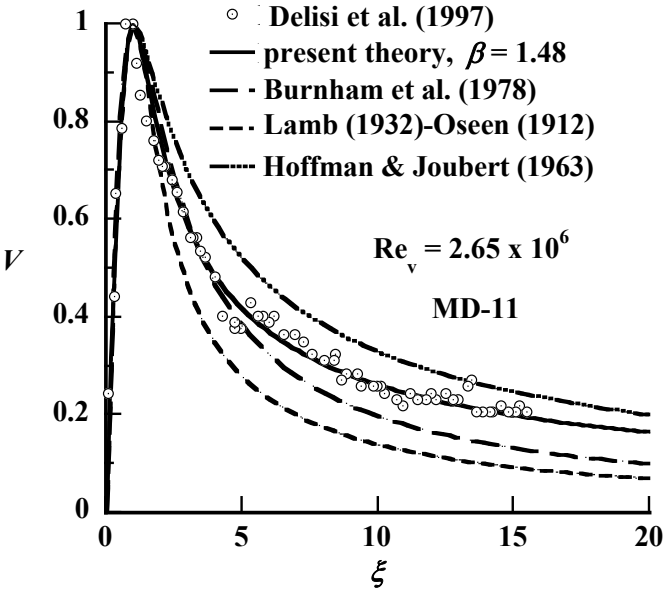

Figure 3.6 Tangential velocity profiles for different vortex models compared to experimental data for and MD-11. Present theory here refers to Eq. (2.18).

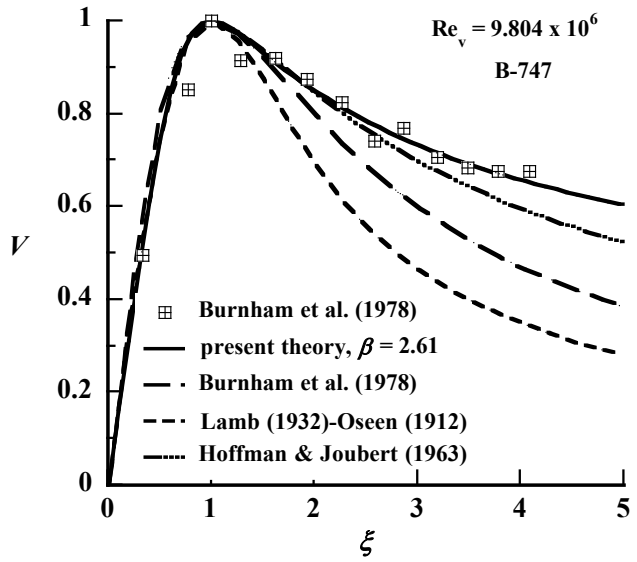

Figure 3.7 Tangential velocity profiles for different vortex models for a B-747. Present theory here refers to Eq. (2.18).

Typical profiles for the radial velocity (u) for both laminar and turbulent vortices obtained using Eq. (2.19) are shown in Fig. (3.8). The profiles of both vortices are negative everywhere, meaning that flow converges toward the center of rotation. In this way, the steady state condition of the vortices is maintained, because the outward diffusion of vorticity is replaced by that brought by the inward fluid convection Vatistas (2004). The axial velocity (h) evolves in a way as to satisfy continuity. The corresponding profiles for h obtained from Eq. (2.20) are given in Fig (3.9).

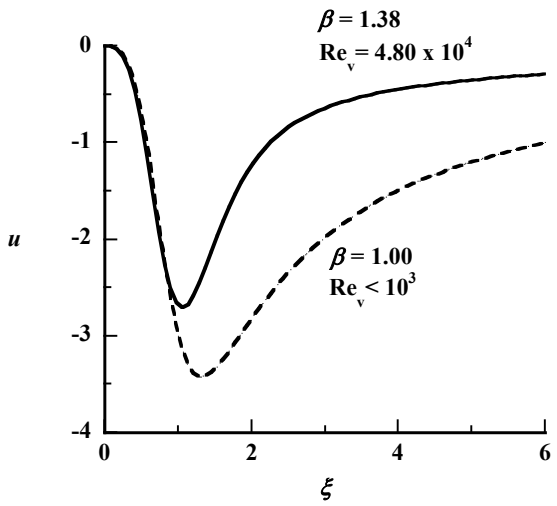

Figure 3.8 Theoretical dimensionless radial velocity distributions for increasing turbulent intensity parameter β. The results were obtained employing Eq. (2.19).

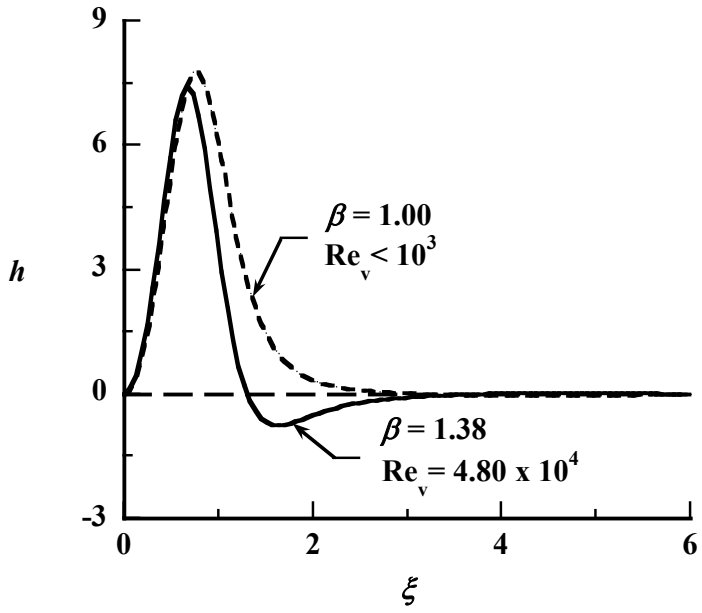

Figure 3.9 Dimensionless axial velocity distributions for increasing turbulent intensity parameter β. The results were obtained employing Eq. (2.20).

3.2 Time decay of turbulent vortices

In chapter 2 (section 2.3) the general formulation for decaying vortices was given. Here the results will be analyzed and compared to observations (when available) starting with the velocity attenuation as a function of time τ or τ'.

The tangential velocity of the decaying vortex can be obtained from Eq. (2.18) and applying the variable transformations as outlined in section 2.3,

$$V(\tau', \xi) = (1+\tau')^{2m-1}(1+\beta)^{m} \frac{\xi}{\left[(1+\tau')^{2} + \beta\,\xi^{4}\right]^{m}} \tag{3.3}$$

Theoretical profiles as a function of time are illustrated in Fig. (3.10) for (a) laminar vortex, and (b) for turbulent vortices.

There are no reliable data to test the effectiveness of Eq. (3.3) in representing turbulent decaying vortices directly. Even for the laminar kind $(\beta = 1)$ there are only two trustworthy datasets that are shown in Figs (3.10) (a) and (b). The vortex begins with a large peak velocity and as the core enlarges the maximum velocity reduces gradually with time. For large radii, all the temporal profiles of circulation tend to free-vortex value.

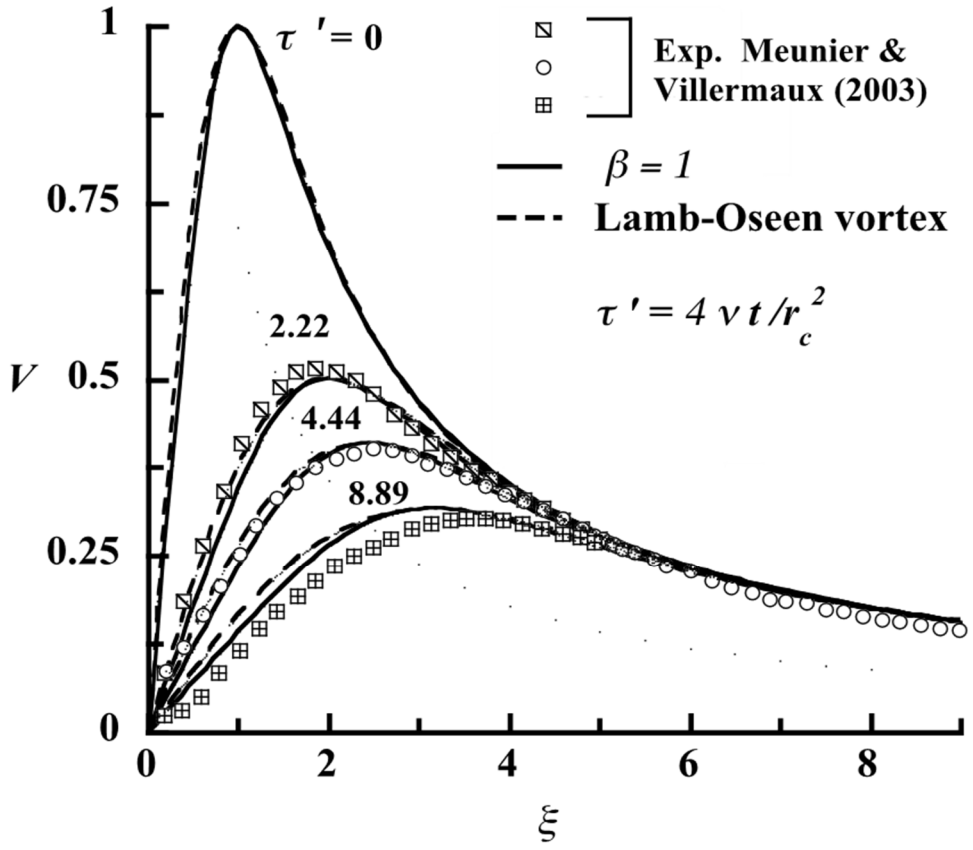
1
0.75
0.5
0.25
0
V
0
2
4
6
8
ξ
τ ′ = 0
2.22
4.44
8.89
Exp. Meunier &
Villermaux (2003)
β = 1
Lamb-Oseen vortex
τ ′ = 4 ν t /r c 2

(a)

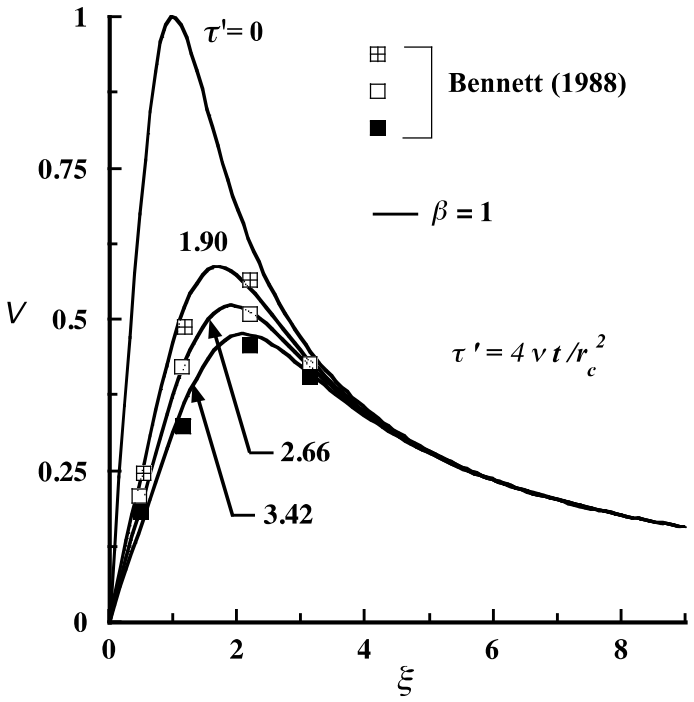

(b)

Figure 3.10. Tangential velocity profile distribution for different timestamps for laminar vortices β=1 (a) Meunier and Villermax (2003), (b) Bennet (1988). The continuous line represents Eq. (2.18).

It is clear that in both cases, Eq. (3.3) represent fairly the physics of the phenomenon.

The decay of a typical turbulent laboratory vortex is shown in Fig. 3.11. In contrast to the laminar decay the far field circulation does not tend to a constant value but rather decreases gradually.

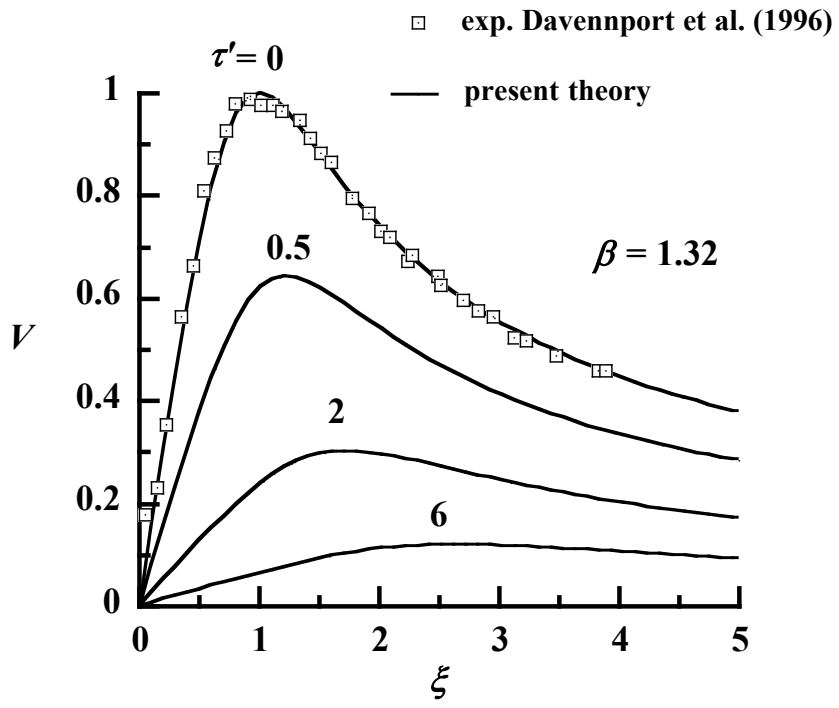

Figure 3.11. Tangential velocity profile distribution for different timestamps for β =1.38. Present theory refers to Eq. (2.18).

In order to calculate the maximum tangential velocity over time, the following simple procedure should be followed. Considering Eq. (2.18) and applying variable transformations as outlined in section 2.3 the tangential velocity for the time decaying vortex is obtained,

$$V(\tau', \xi) = (1+\tau')^{2m-1}(1+\beta)^{m}\frac{\xi}{\left[(1+\tau')^{2}+\beta\,\xi^{4}\right]^{m}} \tag{3.4}$$

Where $m = (1+\beta)/4\beta$, and $\tau = 1+\tau'$.

Taking the partial derivative of V, given by Eq. (3.4), with respect to ξ and setting it to zero will provide the core radius ξ_c as a function of dimensionless time. After considerable algebra we obtain,

$$\xi_c = \sqrt{1+\tau'} \tag{3.5}$$

The same results will be obtained for a Lamb-Oseen laminar vortex. The only difference is in the viscosity term $\left(\tau = 1+\tau' = 1+4\nu t / r_c^2\right)$. For the decaying laminar vortex the kinematic viscosity will be ν while for the turbulent ν_{eff} (note that $\nu < \nu_{eff}$).

Inserting ξ_c from Eq. (3.3) into (3.2), the temporal change of the maximum tangential velocity, is obtained,

$$V_{\max}(\tau, \xi_c) = \frac{1}{\sqrt{1+\tau'}} \tag{3.6}$$

Once again the same relationship will be obtained for a Lamb-Oseen laminar vortex. Detailed derivations for Eqs. (3.5) and (3.6), can be found in Appendix B.

The core expansion and the decay of the maximum velocity for different laminar and turbulent vortices are given in Fig. 3.13.

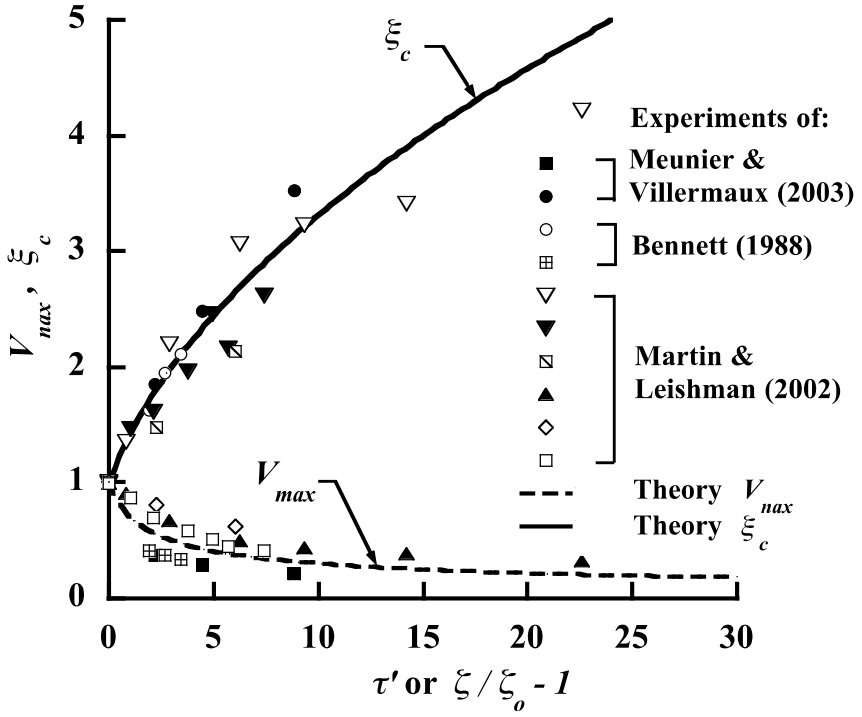

Figure 3.12. Core expansion and maximum velocity decrease over time (or age history $\zeta / \zeta_o - 1$) for various laminar and turbulent decaying vortices. The theory refers to Eq. (3.4) for ξ_c and Eq. (3.5) for $V_{\max}$.

Considering the experimental difficulties associated with temporal event, especially with helicopter rotor blades where the vortex central line is curved, the agreement is indeed reasonable. As time progresses the maximum velocity decreases and the vortex core expands. The vortex Reynolds number, defined as $\mathrm{Re}_v = V_{\theta\max} r_c / \nu$ remains the same because the decrease in velocity is counterbalanced by augmentation of the core size. Thus, here we conjecture that if a vortex starts turbulent it will remain turbulent throughout the decaying process.

3.3 Time decay of turbulent vortices of aircrafts

The wake vortex decay in commercial transport aircrafts is important for the assessment of the hazardous conditions. The dimensional velocity profile can be obtained from Eq. (3.4),

$$V_\theta = \frac{(1+\beta)^m \left(1+4\frac{\nu t}{r_c^{\,2}}\right)^{2m-1} r\, V_{\theta\max}}{\left[\left(1+4\frac{\nu t}{r_c^{\,2}}\right)^2 + \beta\left(\frac{r}{r_c}\right)^4\right]^m r_c} \tag{3.7}$$

Figs. (3.13) and (3.14) shows the predicted reduction of the velocity for two aircraft B-757 and MD-11.

Vortex half-life is defined, as the time required for the maximum tangential velocity to become half of its initial value. The root of the following equation will provide this information,

$$\left\{ \frac{(1+\beta)^m \left(1+4\frac{\nu t}{r_c^{\,2}}\right)^{2m-1} r}{\left[\left(1+4\frac{\nu t}{r_c^{\,2}}\right)^2 + \beta\left(\frac{r}{r_c}\right)^4\right]^m r_c} - \frac{1}{2} \right\} V_{\theta\max} = 0 \tag{3.7}$$

The half time for the two aircraft is given in Figs. (3.14) and (3.15). Based on these results one sees that the half-life (when the maximum velocity becomes half of its initial value) of the wake vortex of the smaller B-757 is less than the larger plane MD-11. The last is qualitatively consistent of what it is expected.

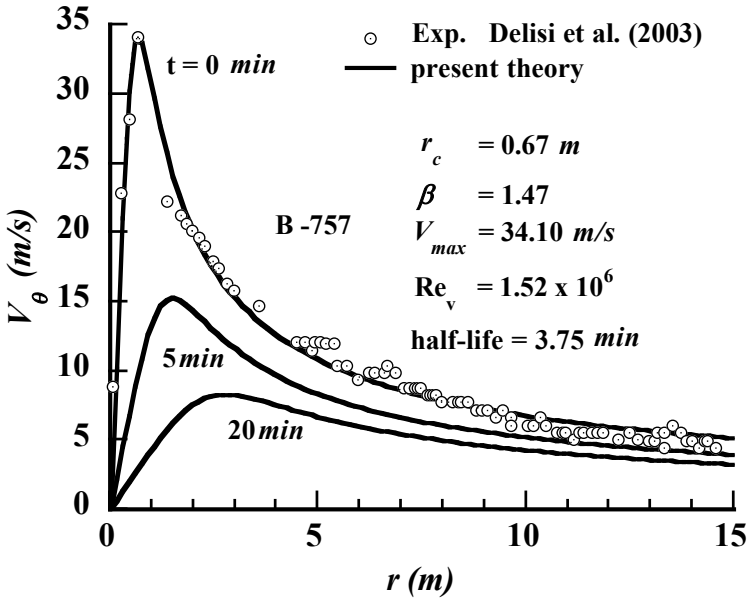

Figure 3.13. Tangential velocity decay for a Boeing B-757. Present theory refers to the dimensional version of Eq. (2.18).

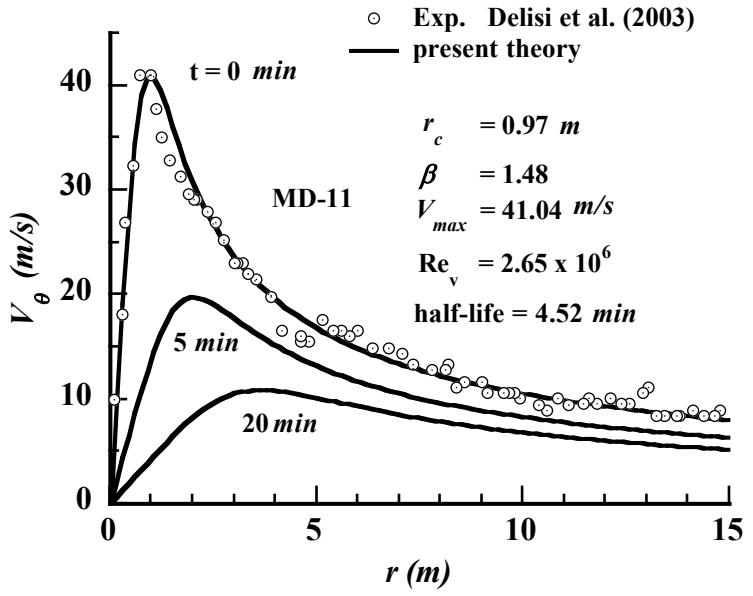

Figure 3.14. Tangential velocity decay for a McDonald Douglas MD-11. Present theory refers to the dimensional version of Eq. (2.18).

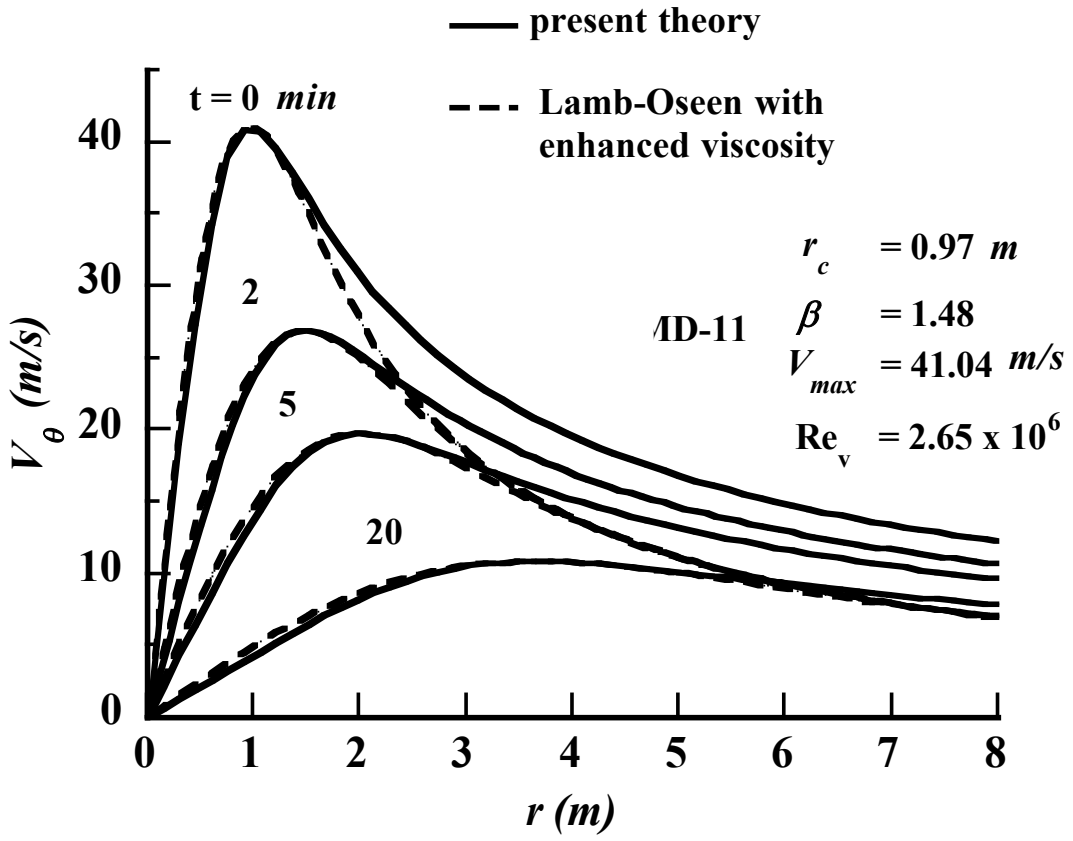

Figure 3.15. Tangential velocity profile decay for a large aircraft compared to enhanced viscosity Lamb-Oseens model. Present theory refers to Eq. (2.18) while the Lab-Oseen refers to the same equation with $\beta = 1$.

Previously, the determination of the vortex circulation at large radius was deemed to be a defining factor in assessing the hazard of commercial transport aircraft. It was thought that the equation that relates the initial circulation strength at large radius (Γ_{mas}), the wingspan, the mass of the aircraft and velocity was considered a good measure to determine the threat. On the other hand, there are some serious drawbacks in this approach. First of all the previous owes its existence on Squire's and Iversen's hypothesis that the circulation for large radius (above $7 \times r_c$) is constant.

This is true for laminar vortices see Fig. 3.16, but for the turbulent kind, as Figs. 3.17 and 3.18 show, it is definitely not the case.

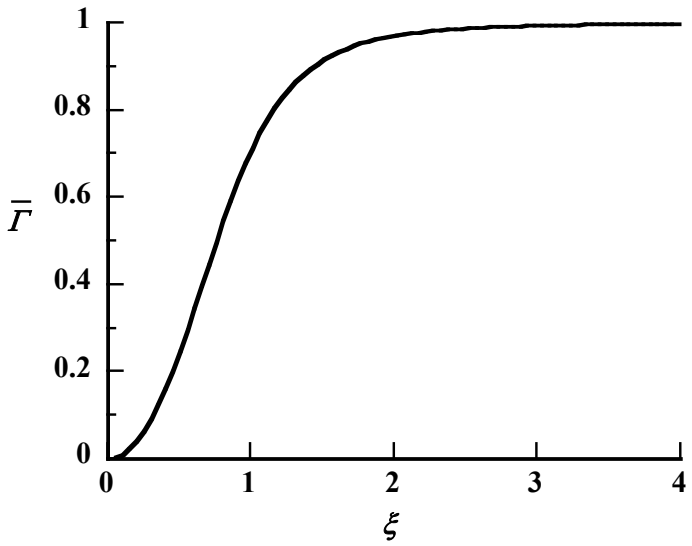

Figure 3.16. The dimensionless circulation $\overline{\Gamma} = \Gamma / \Gamma_{\infty}$ with the dimensionless radius ξ for laminar case.

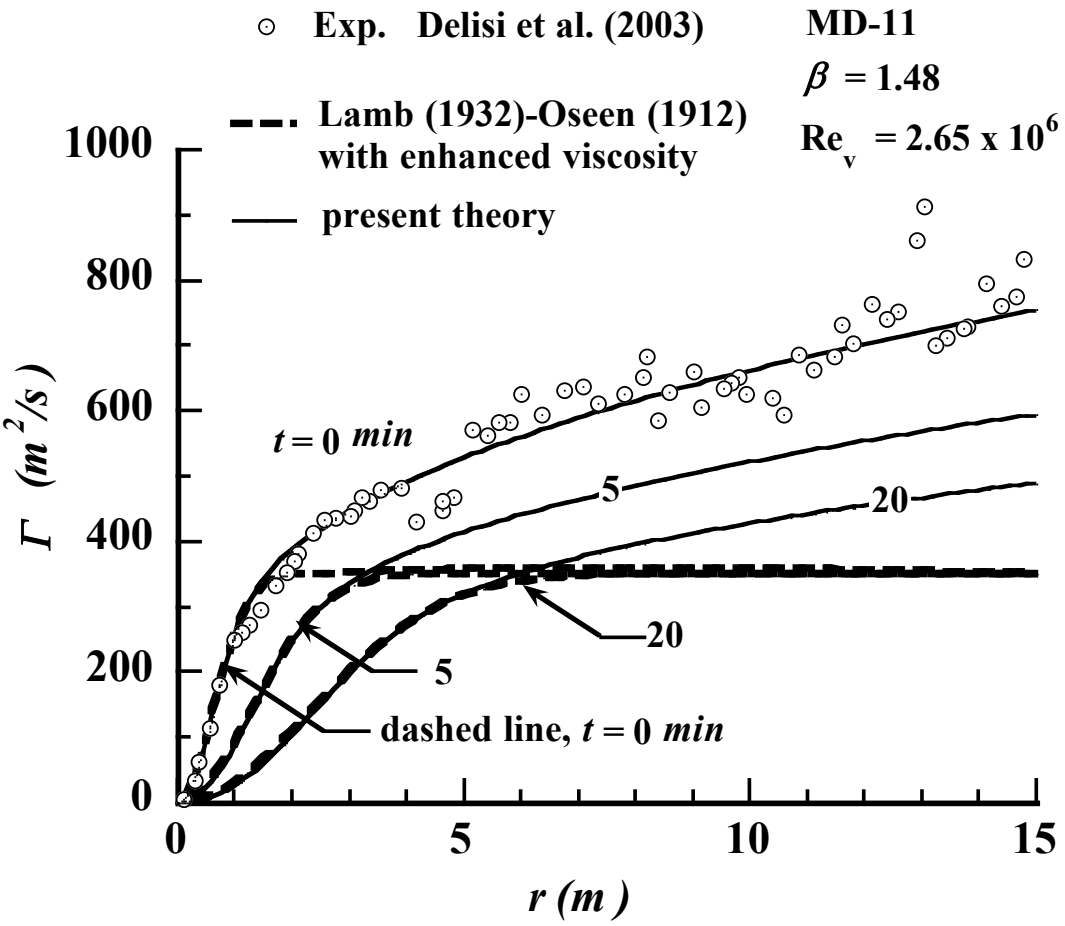

Figure 3.17. Vortex circulation decay for a Boeing B-757 aircraft. Present theory refers to the dimensional tangential velocity, multiplied by 2π times the radius.

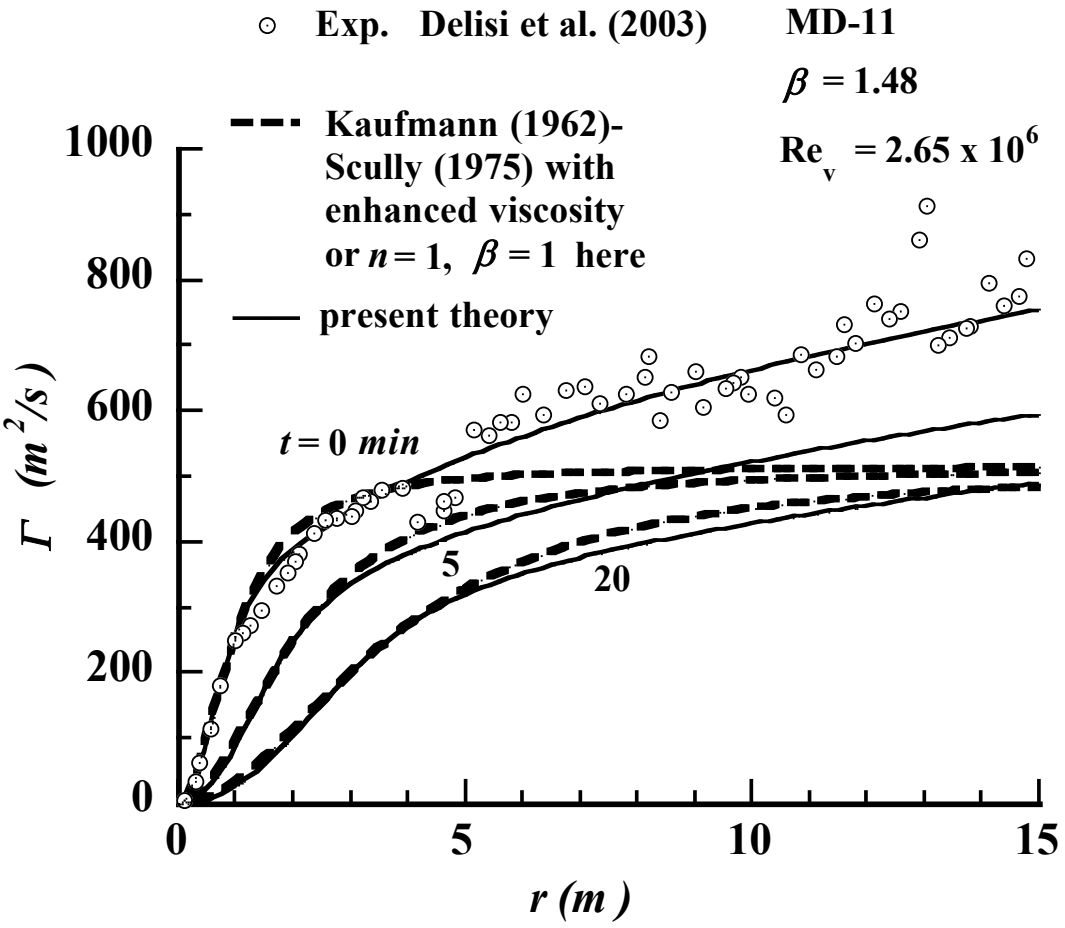

Figure 3.18. Vortex circulation decay for a McDonald Douglas MD-11 aircraft. Present theory refers to Eq. (3.8).

The circulation is

$$V_\theta = \frac{(1+\beta)^m \left(1+4\frac{\nu t}{r_c^2}\right)^{2m-1} r\, V_{\theta\max}}{\left[\left(1+4\frac{\nu t}{r_c^2}\right)^2 + \beta\left(\frac{r}{r_c}\right)^4\right]^m r_c} \tag{3.8}$$

The circulation $\Gamma \to \infty$, as $r \to \infty$ and therefore Γ becomes unbounded making the circulation not to be an effective property in assessing the dangers associated with the vortex wake as was assumed

for example in the model of Burnham-Hallock (1982). A better approach in establishing a model for the hazard will emerge if the circulation is replaced by the tangential velocity. The destabilizing force-rolling moment will be obtained if we integrate the square of the tangential velocity over the wingspan of the following aircraft.

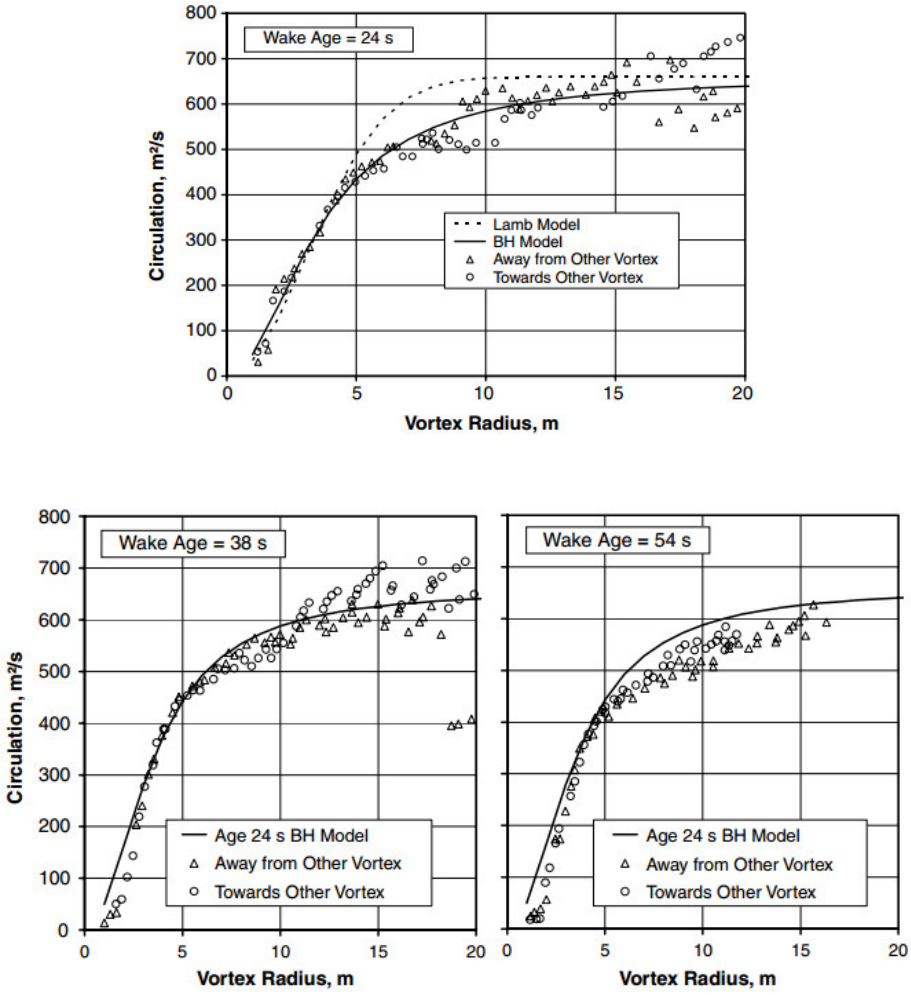

Figure 3.19 Burnham and Hallock (2013) circulation decay for different times (t =24s, t =38s, and t=54s) with radius.

Conclusions

Based on the n-family of vortices (Vatistas et al. (1991)), a new generalized model, which describes both laminar and turbulent vortices, was constructed. Founded on the variable transformation of Vatistas and Aboelkassem (2006), via the Boltzmann's (1894) variable that combines space and time, the model was also expanded to include the time decay phase. An empirical formula that correlated the turbulent intensity parameter with the effective vortex Reynolds number was constructed.

The newly developed simple model, applicable to both laminar and turbulent, steady and decaying vortices was presented and discussed. The tangential velocity profile was accepted by induction. Based on continuity and Navier-Stokes equations the radial and axial velocity components were then obtained solving for the azimuthal momentum and continuity equations respectively. Comparisons of the new model of the tangential velocity profile with various experimental measurements for laminar and turbulent vortex were made and found to correlate fairly well.

The LSE method employed to the several experimental data, furnished the turbulent intensity parameter as a function of the effective Reynolds number. Then an empirical equation was developed to relate the coherent of these two properties. This simplified the procedure of representing the turbulent vortex characteristics as it now allows researchers to approximate the tangential, axial and radial component using only three parameters: the effective Reynolds number, the core radius and the maximum tangential velocity.

Following the variable transformation of Vatistas and Aboelkassem (2006), the steady turbulent vortices were transformed into the corresponding time decaying version. The

applicability of the time decaying model was gaged by comparing the results to numerous cases of actual vortices with high turbulent intensity. In addition, aircraft wake and helicopter blade tip-vortices, which are turbulent, were compared to the new model's predictions and found to relate well. The circulation profiles that are widely used in aviation today to define the hazard threshold of the aircraft spacing system in large airports were found to be insufficient in representing the real case as the assumed flattening of the curve for large radial distances, applicable to laminar cases, does not apply in the case of turbulent vortices. Consequently, the radius of a specific number times the core, to represent the circulation at "infinity", proposed by Squire (1965) and Iversen (1976) and followed by numerous other models like Burnham and Hallock (1982) Proctor (2000) should be re-evaluated. Therefore, future work should focus on the correlation of vortex hazard threshold on the tangential velocity instead of its circulation signature.

Future work

There are several areas in which the determination of safe separation distance of aircrafts could be improved.

The wake hazard threshold can be defined as the wind loading, that a specific following aircraft, can overcome the rolling moment. The most hazardous situation is associated with induced rolling moments that can exceed the stability performance characteristics of the succeeding aircraft. The wingspan of the encountering airplane plays a primary role in the aircraft's ability to overcome the hazard. Furthermore, the counter-control of the following aircraft is effective only in cases where the wingspan of the following aircraft extends beyond the rotational flow field of the wake vortex. In a case similar to the mentioned before, a simplistic approach to define the dangerous threshold lies on the calculation of the wind load that the vortex up-wash and down-wash apply on the aircraft. If the wing is assumed to a flat plate with drag coefficient C_d (normal to the flow, say equal to 1.9) then the drag force can be expressed as:

$$F_d = \frac{1}{2} C_d \, \rho \; c \int_0^L V^2 dr$$

From the free body diagram shown in Fig 3.20 assuming that the center of gravity passes through the center roll axis of the fuselage, the encountered rolling moment will be,

$$M = F_d \, 2 \, l$$

If this value is larger than the maximum moment for stability, then the aircraft will not recover. Of course the human factor (pilot) must also be entered into the calculations as well as meteorological data.

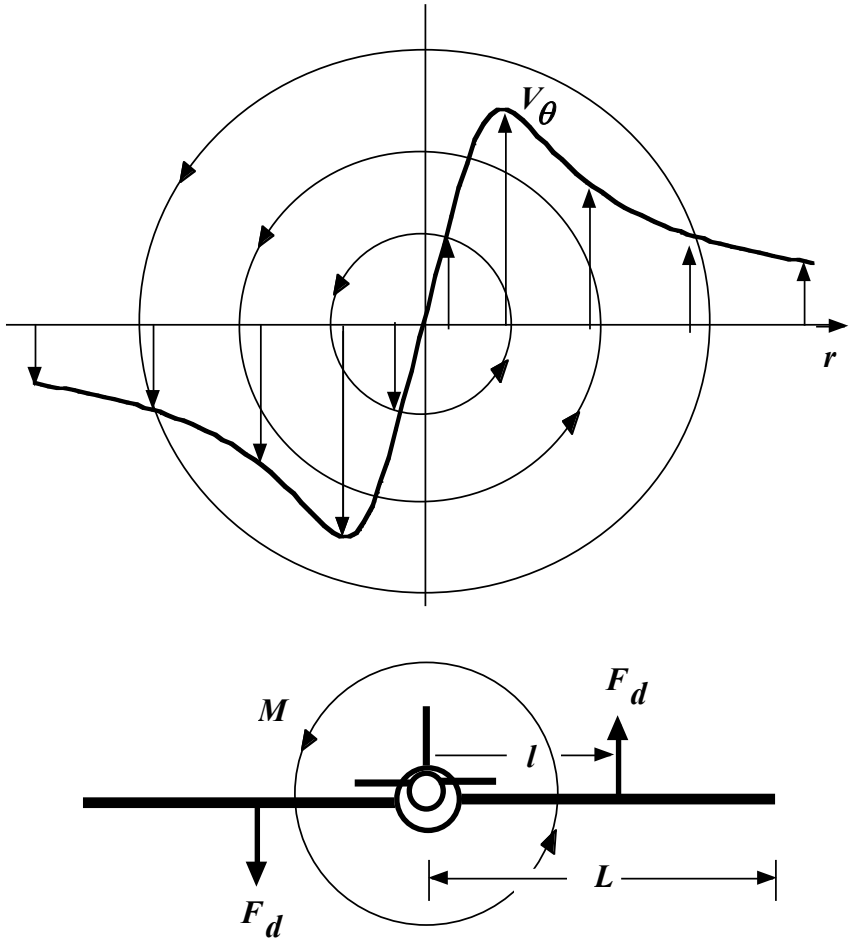

Figure 3.20. Schematic of the assumed following smaller aircraft hazardous encounter.

On the experimental side, reliable full-scale data using modern methods and techniques to characterize the tangential velocity radial profile as a function of time must be collected. This is

especially true for the case of very large planes such as the Boing B-747 and the Airbus A-380 where the present data are either not reliable (B-747) or nonexistent (A-380).

Future, full-scale computational fluid dynamics solution of an entire aircraft could furnish the required details of wing tip vortices. The present simple approach could be useful in the validation of the results.

References

Aboelkassem Y.andVatistas,G.H. (2007) “New Model for Compressible Vortices,” J. Fluid Eng. Vol. 29, pp.1073-1079.

Ansari S. A., Zbikowski, R., and Knowles, A. (2006) “Non-Linear Unsteady Aerodynamic Model for Insect-Like Flapping Wings in the Hover. Part 2: Implementation and Validation,” Journal of Aerospace Engineering, Vol. 220, No. 3, pp. 169–186.

Antonini E. G. A., Bedon, G., De Betta, S., Michelini, L., Marco Raciti Castelli, M. R., and Benini, E. (2015) “Innovative Discrete-Vortex Model for Dynamic Stall Simulations,” AIAA Journal, Vol. 53, No. 2, pp. 479–485.

Bennett T. J. (1988) “Vortex Coalescence and Decay,” Ph.D. dissertation, Department of Civil and Environmental Engineering, Washington State University, Pullman, Wash. USA.

Bhagwat M. J., and Leishman, J. G. (2000) “Correlation of Helicopter Tip Vortex Measurements,” AIAA Journal, Vol. 38, No. 2, 2000, pp. 301–308.

Bhagwat M. J., and Leishman, J. G. (2002) “Viscous Vortex Core Models for

Free-Vortex Wake Calculations,” Proceedings of the 58th Annual Forum of the American Helicopter Society International, 11–13, June 2002.

Bhagwat M. J., and Leishman, J. G. (2000)[b] “Measurements of Bound and Wake Circulation on a Helicopter Rotor,” Journal of Aircraft, Vol. 37, No. 2, 2000, pp. 227–234.

Boltzmann L., “Zur Integration der Diffusionsgleichung bei Variabeln Diffusions-coefficienten,” Annalen der Physik, Vol. 53, 1894, pp. 959–964.

Brix S., Neuwerth, G., and Jacob, D., (2000) “The Inlet-Vortex System of Jet Engines Operating Near the Ground,” AIAA Paper 2000-3998.

Burnham D.C., Hallock, J.N. (2013) “Decay Characteristics of Wake Vortices from Jet Transport

Aircraft," Journal of aircraft, Vol. 50, No. 1, pp. 82-87.

Burnham D.C., Hallock, J.N. (1982) "Chicago Monostatic Acoustic Vortex Sensing System," U.S. Department of Transportation, DOT-TSC-FAA-79-103, 206 p.

Burnham D. C., Hallock, J. N., Tombach, I. H., Brashears, M. R. and Barber, M. R. (1978) "Ground-Based Measurements of the Wake Vortex Characteristics of a B-747 Aircraft in Various Configurations," Dept. of Transportation, Transportation Systems Center Rept. FAA-RD-78-146, Cambridge, MA.

Burgers J. M. (1948) ''A Mathematical Model Illustrating the Theory of Turbulence,'' Advances in Applied Mechanics, Vol. 1, pp. 171– 199.

Caradonna F. X., and Tung, C. (1981) "Experimental and Analytical Studies of a Model Helicopter Rotor," Vertica, Vol. 5, pp. 149–161.

Cotel A. J., and Breidenthal, R. E. (1999) "Turbulence inside a Vortex," Physics of Fluids, Vol. 11, No. 10, pp. 3026–3029.

Davenport W. J., Rife, M. C., Liapis, S. I., and Follin, G. J. (1996) "The Structure and Development of a Wing-tip Vortex," Journal of Fluid Mechanics, Vol. 312, pp. 67–106.

Delisi D. P., Greene, G. C., Robins, R. E., Vicroy, D. C., and Wang, F. Y. (2003) "Aircraft Wake Vortex Core Size Measurements," 21st Applied Aerodynamics Conference, AIAA Paper 2003-3811.

Dosanjh D. S., Gasparek, E. P. and Eskinazi, S. (1962) "The Decay of a Viscous Trailing Vortex," Aeronautical Quarterly, 13 (2), pp. 167–188.

Grifiths R. W., and Hopfinger, E. J. (1987) "Coalescing of Geostrophic Vortices," Journal of Fluid Mechanics, Vol. 178, pp. 73–97.

Han Y. O., Leishman, J. G. and Coyne, A. J. (1997) "On the Turbulent Structure of a Tip Vortex Generated by a Rotor," AIAA Journal, Vol. 35, No. 3, March 1997,pp. 477–485.

Haw P. (1969) "The Analogy Between Streamline Curvature and Buoyancy in Turbulent Shear

Flows," Journal of Fluid Mechanics, Vol. 36, pp. 177–191.

Hinton D. A. and Tatnall C. R. (1997) "A Candidate Wake Vortex Strength Definition for Application to the NASA Aircraft Vortex Spacing System (AVOSS)," NASA Technical Memorandum 110343.

Holzapfel A. Hofbauer, T., Gerz, T., and Schumann, U. (2001) "Aircraft Wake Vortex Evolution and Decay in Idealized and Real Environtments: Methodologies, Benefits and Limitations," Proceedings of the Euromech Colloquium, 2001.

Holforty L. W. (2003) "Flight-Dec Display of Neighboring Aircraft Vortices", PhD. Thesis, Department of Aeronautics and Astronautics, Stanford University, USA.

Hoffman E. R., and Joubert P. N. (1963) "Turbulent Line Vortices," Journal of Fluid Mechanics, Vol. 16, 1963, pp. 395–411.

Iversen J. D. (1973) "Correlation of Turbulent Trailing Vortex Decay Data," Journal of Aircraft, Vol. 13, No. 5, pp. 338-342.

Kaufmann W. (1962) "Über die Ausbreitung kreiszylindrischer Wirbel in zähen (viskosen) Flüssigkeiten." Ingenieur-Arch. Vol. 31, No1, PP. 1- 9.

Koval P.V. and Michaelov, P. S. (1972) "Velocity and Pressure Distributions of Liquid in a Swirl Chamber." Teploenergetica, vol.19, no.2, pp. 25-28.

Kecskemety K. M., and McNamara, J. J., (2011) "Influence of Wake Effects and Inflow Turbulence on Wind Turbine Loads," AIAA Journal, Vol. 49, No. 11, pp. 2564–2576.

Lamb H., (1932)"Hydrodynamics," 6th ed., Cambridge Univ. Press, New York, pp. 591-592.

Leishman J. G., (1998) "Measurements of the Aperiodic Wake of a Hovering Rotor," Experiments in Fluids, Vol. 25, No. 4, pp. 352–361.

Lundgren T. S. (1982) "Strained spiral vortex model for turbulent fine structure," Physics of Fluids, Vol. 25, No. 12, pp. 2193-2203.

Martin P., and Leishman, J. G., (2002) “Trailing Vortex Measurements in the Wake of a Hovering Rotor with Various Tip Shapes,” Proceedings of the 58th Annual Forum of the American Helicopter Society International, Montreal Canada, June 11–13, 2002.

Martin P. B., Pugliese, G., and Leishman, J. G., (2001) “High Resolution Trailing Vortex Measurements in the Wake of a Hovering Rotor,” American Helicopter Society 57th Annual National Forum, Washington, DC, May 9–11.

Mahalingam R., and Komerath, N. M., (1998) “Measurements of the Near Wake of a Rotor in Forward Flight,” AIAA Paper 98-0692.

McAlister K. W., (1996) “Measurements in the Near Wake of a Hovering Rotor,” AIAA Paper 96-1958.

McCormick B. W., Tangler, J. L., and Sherrieb, H. E., (1968) “Structure of Trailing Vortices,” Journal of Aircraft, Vol. 5, No. 3, pp. 260–267.

Meunie, P., and Villermaux, E., (2003) “How Vortices Mix,” Journal of Fluid Mechanics, Vol. 476, pp. 213–222.

Murphy J. P., and MacManus, D. G. (2011) “Ground Vortex Aerodynamics Under Crosswind Conditions,” Experiments in Fluids, Vol. 50, No. 1, 2011, pp. 109–124.

Murphy J. P., and MacManus, D. G. (2011) “Inlet Ground Vortex Aero- dynamics Under Headwind Conditions,” Aerospace Science and Technology, Vol. 15, No. 3, pp. 207–215.

Newman B. G. (1959) “Flow in a Viscous Trailing Vortex,” Aeronautical Quarterly, 10 (2), pp. 149–162.

Osseen C. W. (1912) “Uber Wirbelbewegune in Einer Reiben-den Flussigkeit,” Arkiv för Matematik, Astronomi och Fysik, Vol. 7, pp. 14–21.

Proctor F.H., Hamilton, D.W. and Han, J. (2000) "Wake Vortex Transport and Decay in Ground Effect: Vortex Linking with the Ground", AIAA Paper 2000-0757.

Ramasamy M. and Leishman, J. G. (2007) “A Reynolds Number-Based Blade Tip Vortex

Model," Journal of the American Helicopter Society, Vol. 52, Issue 3, pp. 214–223.

Ramesh K., Murua, J., and Gopalarathnam, A., "Limit-Cycle Oscillations in Unsteady Flows Dominated by Intermittent Leading-Edge Vortex Shedding," Journal of Fluids and Structures, Vol. 55, May 2015, pp. 84–105.

Rankine W. J. M. (1858) "Manual of Applied Mechanics," C. Griffen Co., London, 1858, pp. 576–578.

Rossow V. J. (2006) "Origin of Exponential Solution for Laminar Decay of Isolated Vortex," Journal of Aircraft, Vol. 43, No. 3, pp. 709-712.

Scully M. P. (1975) "Computation of Helicopter Rotor Wake Geometry and Its Influence on Rotor Harmonic Airloads," Aeroelastic and Structures Research Lab., Massachusetts Inst. of Technology TR ASRL TR-178-1, Cambridge, MA, March.

Snedeker R. S. (1972) "Effect of Air Injection on the Torque Produced by a Trailing Vortex," Journal of Aircraft, Vol. 9, No. 9, pp. 682–684.

Squire H.B. (1965) "The Growth of a Vortex in Turbulent Flow," Aeronautical Quarterly, Vol. 16, Part 3, August 1965, pp. 302-306.

Sullivan R. D. (1959) "A Two-Cell Vortex Solution of the Navier-Stokes Equations," Journal of the Aerospace Sciences, Vol. 26, pp. 767-768.

Takahashi R. K., and McAlister, K. W. (1987) "Preliminary Study of a Wing- Tip Vortex Using Laser Velocimetry," NASA TM-88343.

Tao S., Jianfeng, T., and Haowen, W., (2013) "Investigation of Rotor Control System Loads," Chinese Journal of Aeronautics, Vol. 26, No. 5, pp. 1114–1124.

Tung C., Pucci, S. L., Caradonna, F. X., and Morse, H. A., "The Structure of Trailing Vortices Generated by Model Helicopter Rotor Blades," NASATM 81316, 1981.

Vatistas G. H., (2006) "Simple Model for Turbulent Tip Vortices," Journal of Aircraft, Vol. 43, No. 5, pp. 1577–1579.

Vatistas H. G., and Aboelkassem, Y., (2006) "Space-Time Analogy of Self-Similar Intense Vortices," AIAA Journal, Vol.44, No. 4, pp. 912-917.

Vatistas, G. H. (1998) "New Model for Intense Self-Similar Vortices." Journal of Propulsion and Power, Vol. 14, No. 4, pp. 462–469.

Vatistas G. H., Kozel, V., and Mih, W. (1991) "A Simpler Model for Concentrated Vortices," Experiments in Fluids, Vol. 11, No. 1, pp. 73–76.

Vatistas G.H., Panagiotakakos, G. D. and Manikis, F. I. (2015) "Extension of the n-Vortex Model to Approximate the Effects of Turbulence," Journal of Aircraft, Vol. 52, No. 5, pp. 1721-1725.

Vatistas G.H. (2004) "The fundamental properties on the n = 2 vortex model." Trans. Canadian Society of Mechanical Engineers, Vol. 28, pp. 43-58.

Wang Y. and Jiang, C. (2010) "Investigation of the Surface Vortex in a Spillway Tunnel Intake," Tsinghua Science and Technology, Vol. 15, No. 5, pp. 561–565.

Zheng T. H., Vatistas, G.H., and Povitsky, A. (2007) "Sound Generation by a Street of Vortices in a Non uniform Flow," Physics of Fluids, Vol. 19, 03710.

.

Appendix A

Boeing 757 Turbulent intensity parameter

```
> E := add( ( V[i] - ξ[i]*( (1 + b)/(b*ξ[i]^4 + 1) )^( (1 + b)/(4*b) ) )^2, i = 1 .. 78 ) :
> diff(%, b) :
```

$$
\begin{aligned}
&subs\Big(\Big(V_1 = 0.24339, V_2 = 0.65854, \xi_1 = 0.19465, \xi_2 = 0.40943, V_3 = 0.82467, V_4 = 1, V_5 \\
&= 0.89837, V_6 = 0.78782, V_7 = 0.67697, V_8 = 0.63061, V_9 = 0.60297, V_{10} = 0.61218, V_{11} \\
&= 0.59376, V_{12} = 0.59376, V_{13} = 0.56583, V_{14} = 0.51976, V_{15} = 0.49212, V_{16} = 0.45498, \\
&V_{17} = 0.43655, V_{18} = 0.41813, V_{19} = 0.40862, V_{20} = 0.38098, V_{21} = 0.34383, V_{22} \\
&= 0.33463, V_{23} = 0.34383, V_{24} = 0.33462, V_{25} = 0.33432, V_{26} = 0.29747, V_{27} = 0.27902, \\
&V_{28} = 0.26051, V_{29} = 0.26969, V_{30} = 0.27887, V_{31} = 0.28802, V_{32} = 0.27875, V_{33} \\
&= 0.25103, V_{34} = 0.26024, V_{35} = 0.25097, V_{36} = 0.24172, V_{37} = 0.24166, V_{38} = 0.23239, \\
&V_{39} = 0.22309, V_{40} = 0.21382, V_{41} = 0.21376, V_{42} = 0.20446, V_{43} = 0.18597, V_{44} \\
&= 0.17670, \xi_3 = 0.057044, \xi_4 = 1, \xi_5 = 1.0538, \xi_6 = 1.3758, \xi_7 = 1.6446, \xi_8 = 1.9666, \xi_9 \\
&= 2.1277, \xi_{10} = 2.6107, \xi_{11} = 2.6107, \xi_{12} = 2.9327, \xi_{13} = 3.1484, \xi_{14} = 3.5236, \xi_{15} \\
&= 3.8456, \xi_{16} = 4.0598, \xi_{17} = 4.4365, \xi_{18} = 4.7053, \xi_{19} = 5.0273, \xi_{20} = 5.5635, \xi_{21} \\
&= 6.4232, \xi_{22} = 6.8531, \xi_{23} = 7.3361, \xi_{24} = 7.6035, \xi_{25} = 7.8191, \xi_{26} = 7.8723, \xi_{27} \\
&= 8.2490, \xi_{28} = 8.4632, \xi_{29} = 8.7852, \xi_{30} = 9.0541, \xi_{31} = 9.6449, \xi_{32} = 9.9123, \xi_{33} \\
&= 10.181, \xi_{34} = 10.181, \xi_{35} = 10.397, \xi_{36} = 10.611, \xi_{37} = 10.880, \xi_{38} = 11.202, \xi_{39} \\
&= 11.632, \xi_{40} = 11.954, \xi_{41} = 12.221, \xi_{42} = 12.651, \xi_{43} = 12.973, \xi_{44} = 13.242, \xi_{45} \\
&= 13.456, \xi_{46} = 13.725, \xi_{47} = 13.940, \xi_{48} = 14.208, \xi_{49} = 14.534, \xi_{50} = 14.956, \xi_{51} \\
&= 15.066, \xi_{52} = 15.382, \xi_{53} = 15.656, \xi_{54} = 15.871, \xi_{55} = 16.029, \xi_{56} = 16.360, \xi_{57} \\
&= 16.576, \xi_{58} = 16.676, \xi_{59} = 16.949, \xi_{60} = 16.949, \xi_{61} = 17.323, \xi_{62} = 17.639, \xi_{63} \\
&= 17.913, \xi_{64} = 18.344, \xi_{65} = 18.502, \xi_{66} = 18.833, \xi_{67} = 18.876, \xi_{68} = 19.149, \xi_{69} \\
&= 19.307, \xi_{70} = 19.580, \xi_{71} = 19.839, \xi_{72} = 20.170, \xi_{73} = 20.443, \xi_{74} = 20.817, \xi_{75} \\
&= 20.817, \xi_{76} = 21.075, \xi_{77} = 21.348, \xi_{78} = 21.622, V_{45} = 0.17664, V_{46} = 0.16737, V_{47} \\
&= 0.15813, V_{48} = 0.15807, V_{49} = 0.15801, V_{50} = 0.13949, V_{51} = 0.15795, V_{52} = 0.15789, \\
&V_{53} = 0.14862, V_{54} = 0.13935, V_{55} = 0.14856, V_{56} = 0.14850, V_{57} = 0.14847, V_{58} \\
&= 0.13923, V_{59} = 0.13917, V_{60} = 0.14841, V_{61} = 0.13911, V_{62} = 0.13908, V_{63} = 0.13902, \\
&V_{64} = 0.12972, V_{65} = 0.12969, V_{66} = 0.12966, V_{67} = 0.13887, V_{68} = 0.13881, V_{69} \\
&= 0.13881, V_{70} = 0.14799, V_{71} = 0.12948, V_{72} = 0.12021, V_{73} = 0.12939, V_{74} = 0.11088, \\
&V_{75} = 0.12009, V_{76} = 0.12006, V_{77} = 0.09233, V_{78} = 0.10152\Big), E\Big) :
\end{aligned}
$$

```
>
> DirectSearch:-SolveEquations(%)
```

$$\left[0.460023042327645, \left[\ 0.678249985129115\ \right], [b = 1.35596909079757], 20\right]$$

Error n=1 for B757

```
> E := add( ( V[i] - ξ[i]*( (1 + 1.10865677853798) / ( 1.10865677853798*ξ[i]^2 + 1 ) )^( (1
      + 1.10865677853798) / (2*1.10865677853798) ) )^2, i = 1 .. 78 ) :
>
```

$$subs\Big(\big(V_1 = 0.24339, V_2 = 0.65854, \xi_1 = 0.19465, \xi_2 = 0.40943, V_3 = 0.82467, V_4 = 1, V_5 = 0.89837, V_6 = 0.78782, V_7 = 0.67697, V_8 = 0.63061, V_9 = 0.60297, V_{10} = 0.61218, V_{11} = 0.59376, V_{12} = 0.59376, V_{13} = 0.56583, V_{14} = 0.51976, V_{15} = 0.49212, V_{16} = 0.45498, V_{17} = 0.43655, V_{18} = 0.41813, V_{19} = 0.40862, V_{20} = 0.38098, V_{21} = 0.34383, V_{22} = 0.33463, V_{23} = 0.34383, V_{24} = 0.33462, V_{25} = 0.33432, V_{26} = 0.29747, V_{27} = 0.27902, V_{28} = 0.26051, V_{29} = 0.26969, V_{30} = 0.27887, V_{31} = 0.28802, V_{32} = 0.27875, V_{33} = 0.25103, V_{34} = 0.26024, V_{35} = 0.25097, V_{36} = 0.24172, V_{37} = 0.24166, V_{38} = 0.23239, V_{39} = 0.22309, V_{40} = 0.21382, V_{41} = 0.21376, V_{42} = 0.20446, V_{43} = 0.18597, V_{44} = 0.17670, \xi_3 = 0.057044, \xi_4 = 1, \xi_5 = 1.0538, \xi_6 = 1.3758, \xi_7 = 1.6446, \xi_8 = 1.9666, \xi_9 = 2.1277, \xi_{10} = 2.6107, \xi_{11} = 2.6107, \xi_{12} = 2.9327, \xi_{13} = 3.1484, \xi_{14} = 3.5236, \xi_{15} = 3.8456, \xi_{16} = 4.0598, \xi_{17} = 4.4365, \xi_{18} = 4.7053, \xi_{19} = 5.0273, \xi_{20} = 5.5635, \xi_{21} = 6.4232, \xi_{22} = 6.8531, \xi_{23} = 7.3361, \xi_{24} = 7.6035, \xi_{25} = 7.8191, \xi_{26} = 7.8723, \xi_{27} = 8.2490, \xi_{28} = 8.4632, \xi_{29} = 8.7852, \xi_{30} = 9.0541, \xi_{31} = 9.6449, \xi_{32} = 9.9123, \xi_{33} = 10.181, \xi_{34} = 10.181, \xi_{35} = 10.397, \xi_{36} = 10.611, \xi_{37} = 10.880, \xi_{38} = 11.202, \xi_{39} = 11.632, \xi_{40} = 11.954, \xi_{41} = 12.221, \xi_{42} = 12.651, \xi_{43} = 12.973, \xi_{44} = 13.242, \xi_{45} = 13.456, \xi_{46} = 13.725, \xi_{47} = 13.940, \xi_{48} = 14.208, \xi_{49} = 14.534, \xi_{50} = 14.956, \xi_{51} = 15.066, \xi_{52} = 15.382, \xi_{53} = 15.656, \xi_{54} = 15.871, \xi_{55} = 16.029, \xi_{56} = 16.360, \xi_{57} = 16.576, \xi_{58} = 16.676, \xi_{59} = 16.949, \xi_{60} = 16.949, \xi_{61} = 17.323, \xi_{62} = 17.639, \xi_{63} = 17.913, \xi_{64} = 18.344, \xi_{65} = 18.502, \xi_{66} = 18.833, \xi_{67} = 18.876, \xi_{68} = 19.149, \xi_{69} = 19.307, \xi_{70} = 19.580, \xi_{71} = 19.839, \xi_{72} = 20.170, \xi_{73} = 20.443, \xi_{74} = 20.817, \xi_{75} = 20.817, \xi_{76} = 21.075, \xi_{77} = 21.348, \xi_{78} = 21.622, V_{45} = 0.17664, V_{46} = 0.16737, V_{47} = 0.15813, V_{48} = 0.15807, V_{49} = 0.15801, V_{50} = 0.13949, V_{51} = 0.15795, V_{52} = 0.15789, V_{53} = 0.14862, V_{54} = 0.13935, V_{55} = 0.14856, V_{56} = 0.14850, V_{57} = 0.14847, V_{58} = 0.13923, V_{59} = 0.13917, V_{60} = 0.14841, V_{61} = 0.13911, V_{62} = 0.13908, V_{63} = 0.13902, V_{64} = 0.12972, V_{65} = 0.12969, V_{66} = 0.12966, V_{67} = 0.13887, V_{68} = 0.13881, V_{69} = 0.13881, V_{70} = 0.14799, V_{71} = 0.12948, V_{72} = 0.12021, V_{73} = 0.12939, V_{74} = 0.11088, V_{75} = 0.12009, V_{76} = 0.12006, V_{77} = 0.09233, V_{78} = 0.10152\big), E\Big)$$

0.7229753860

Error n=2 for B757

> $E := add\left(\left(V[i] - \xi[i] * \left((1 + 1.35596909262371)/\left(1.35596909262371 * \xi[i]\text{^}4 + 1\right)\right)\text{^}((1 + 1.35596909262371)/(4 * 1.35596909262371))\right)\text{^}2, i = 1 .. 78\right)$:

>

$$subs\Big(\big(V_1 = 0.24339, V_2 = 0.65854, \xi_1 = 0.19465, \xi_2 = 0.40943, V_3 = 0.82467, V_4 = 1, V_5 = 0.89837, V_6 = 0.78782, V_7 = 0.67697, V_8 = 0.63061, V_9 = 0.60297, V_{10} = 0.61218, V_{11} = 0.59376, V_{12} = 0.59376, V_{13} = 0.56583, V_{14} = 0.51976, V_{15} = 0.49212, V_{16} = 0.45498, V_{17} = 0.43655, V_{18} = 0.41813, V_{19} = 0.40862, V_{20} = 0.38098, V_{21} = 0.34383, V_{22} = 0.33463, V_{23} = 0.34383, V_{24} = 0.33462, V_{25} = 0.33432, V_{26} = 0.29747, V_{27} = 0.27902, V_{28} = 0.26051, V_{29} = 0.26969, V_{30} = 0.27887, V_{31} = 0.28802, V_{32} = 0.27875, V_{33} = 0.25103, V_{34} = 0.26024, V_{35} = 0.25097, V_{36} = 0.24172, V_{37} = 0.24166, V_{38} = 0.23239, V_{39} = 0.22309, V_{40} = 0.21382, V_{41} = 0.21376, V_{42} = 0.20446, V_{43} = 0.18597, V_{44} = 0.17670, \xi_3 = 0.057044, \xi_4 = 1, \xi_5 = 1.0538, \xi_6 = 1.3758, \xi_7 = 1.6446, \xi_8 = 1.9666, \xi_9 = 2.1277, \xi_{10} = 2.6107, \xi_{11} = 2.6107, \xi_{12} = 2.9327, \xi_{13} = 3.1484, \xi_{14} = 3.5236, \xi_{15} = 3.8456, \xi_{16} = 4.0598, \xi_{17} = 4.4365, \xi_{18} = 4.7053, \xi_{19} = 5.0273, \xi_{20} = 5.5635, \xi_{21} = 6.4232, \xi_{22} = 6.8531, \xi_{23} = 7.3361, \xi_{24} = 7.6035, \xi_{25} = 7.8191, \xi_{26} = 7.8723, \xi_{27} = 8.2490, \xi_{28} = 8.4632, \xi_{29} = 8.7852, \xi_{30} = 9.0541, \xi_{31} = 9.6449, \xi_{32} = 9.9123, \xi_{33} = 10.181, \xi_{34} = 10.181, \xi_{35} = 10.397, \xi_{36} = 10.611, \xi_{37} = 10.880, \xi_{38} = 11.202, \xi_{39} = 11.632, \xi_{40} = 11.954, \xi_{41} = 12.221, \xi_{42} = 12.651, \xi_{43} = 12.973, \xi_{44} = 13.242, \xi_{45} = 13.456, \xi_{46} = 13.725, \xi_{47} = 13.940, \xi_{48} = 14.208, \xi_{49} = 14.534, \xi_{50} = 14.956, \xi_{51} = 15.066, \xi_{52} = 15.382, \xi_{53} = 15.656, \xi_{54} = 15.871, \xi_{55} = 16.029, \xi_{56} = 16.360, \xi_{57} = 16.576, \xi_{58} = 16.676, \xi_{59} = 16.949, \xi_{60} = 16.949, \xi_{61} = 17.323, \xi_{62} = 17.639, \xi_{63} = 17.913, \xi_{64} = 18.344, \xi_{65} = 18.502, \xi_{66} = 18.833, \xi_{67} = 18.876, \xi_{68} = 19.149, \xi_{69} = 19.307, \xi_{70} = 19.580, \xi_{71} = 19.839, \xi_{72} = 20.170, \xi_{73} = 20.443, \xi_{74} = 20.817, \xi_{75} = 20.817, \xi_{76} = 21.075, \xi_{77} = 21.348, \xi_{78} = 21.622, V_{45} = 0.17664, V_{46} = 0.16737, V_{47} = 0.15813, V_{48} = 0.15807, V_{49} = 0.15801, V_{50} = 0.13949, V_{51} = 0.15795, V_{52} = 0.15789, V_{53} = 0.14862, V_{54} = 0.13935, V_{55} = 0.14856, V_{56} = 0.14850, V_{57} = 0.14847, V_{58} = 0.13923, V_{59} = 0.13917, V_{60} = 0.14841, V_{61} = 0.13911, V_{62} = 0.13908, V_{63} = 0.13902, V_{64} = 0.12972, V_{65} = 0.12969, V_{66} = 0.12966, V_{67} = 0.13887, V_{68} = 0.13881, V_{69} = 0.13881, V_{70} = 0.14799, V_{71} = 0.12948, V_{72} = 0.12021, V_{73} = 0.12939, V_{74} = 0.11088, V_{75} = 0.12009, V_{76} = 0.12006, V_{77} = 0.09233, V_{78} = 0.10152\big), E\Big)$$

0.6782499855

Error n=3 for B757

> $E := add\left(\left(V[i] - \xi[i] * \left((1 + 1.44076080998757)/\left(1.44076080998757 * \xi[i]\text{^}6 + 1\right)\right)\text{^}((1 + 1.44076080998757)/(6 * 1.44076080998757))\right)\text{^}2, i = 1 .. 78\right)$:

>

$$subs\Big(\big(V_1 = 0.24339, V_2 = 0.65854, \xi_1 = 0.19465, \xi_2 = 0.40943, V_3 = 0.82467, V_4 = 1, V_5 = 0.89837, V_6 = 0.78782, V_7 = 0.67697, V_8 = 0.63061, V_9 = 0.60297, V_{10} = 0.61218, V_{11} = 0.59376, V_{12} = 0.59376, V_{13} = 0.56583, V_{14} = 0.51976, V_{15} = 0.49212, V_{16} = 0.45498, V_{17} = 0.43655, V_{18} = 0.41813, V_{19} = 0.40862, V_{20} = 0.38098, V_{21} = 0.34383, V_{22} = 0.33463, V_{23} = 0.34383, V_{24} = 0.33462, V_{25} = 0.33432, V_{26} = 0.29747, V_{27} = 0.27902, V_{28} = 0.26051, V_{29} = 0.26969, V_{30} = 0.27887, V_{31} = 0.28802, V_{32} = 0.27875, V_{33} = 0.25103, V_{34} = 0.26024, V_{35} = 0.25097, V_{36} = 0.24172, V_{37} = 0.24166, V_{38} = 0.23239, V_{39} = 0.22309, V_{40} = 0.21382, V_{41} = 0.21376, V_{42} = 0.20446, V_{43} = 0.18597, V_{44} = 0.17670, \xi_3 = 0.057044, \xi_4 = 1, \xi_5 = 1.0538, \xi_6 = 1.3758, \xi_7 = 1.6446, \xi_8 = 1.9666, \xi_9 = 2.1277, \xi_{10} = 2.6107, \xi_{11} = 2.6107, \xi_{12} = 2.9327, \xi_{13} = 3.1484, \xi_{14} = 3.5236, \xi_{15} = 3.8456, \xi_{16} = 4.0598, \xi_{17} = 4.4365, \xi_{18} = 4.7053, \xi_{19} = 5.0273, \xi_{20} = 5.5635, \xi_{21} = 6.4232, \xi_{22} = 6.8531, \xi_{23} = 7.3361, \xi_{24} = 7.6035, \xi_{25} = 7.8191, \xi_{26} = 7.8723, \xi_{27} = 8.2490, \xi_{28} = 8.4632, \xi_{29} = 8.7852, \xi_{30} = 9.0541, \xi_{31} = 9.6449, \xi_{32} = 9.9123, \xi_{33} = 10.181, \xi_{34} = 10.181, \xi_{35} = 10.397, \xi_{36} = 10.611, \xi_{37} = 10.880, \xi_{38} = 11.202, \xi_{39} = 11.632, \xi_{40} = 11.954, \xi_{41} = 12.221, \xi_{42} = 12.651, \xi_{43} = 12.973, \xi_{44} = 13.242, \xi_{45} = 13.456, \xi_{46} = 13.725, \xi_{47} = 13.940, \xi_{48} = 14.208, \xi_{49} = 14.534, \xi_{50} = 14.956, \xi_{51} = 15.066, \xi_{52} = 15.382, \xi_{53} = 15.656, \xi_{54} = 15.871, \xi_{55} = 16.029, \xi_{56} = 16.360, \xi_{57} = 16.576, \xi_{58} = 16.676, \xi_{59} = 16.949, \xi_{60} = 16.949, \xi_{61} = 17.323, \xi_{62} = 17.639, \xi_{63} = 17.913, \xi_{64} = 18.344, \xi_{65} = 18.502, \xi_{66} = 18.833, \xi_{67} = 18.876, \xi_{68} = 19.149, \xi_{69} = 19.307, \xi_{70} = 19.580, \xi_{71} = 19.839, \xi_{72} = 20.170, \xi_{73} = 20.443, \xi_{74} = 20.817, \xi_{75} = 20.817, \xi_{76} = 21.075, \xi_{77} = 21.348, \xi_{78} = 21.622, V_{45} = 0.17664, V_{46} = 0.16737, V_{47} = 0.15813, V_{48} = 0.15807, V_{49} = 0.15801, V_{50} = 0.13949, V_{51} = 0.15795, V_{52} = 0.15789, V_{53} = 0.14862, V_{54} = 0.13935, V_{55} = 0.14856, V_{56} = 0.14850, V_{57} = 0.14847, V_{58} = 0.13923, V_{59} = 0.13917, V_{60} = 0.14841, V_{61} = 0.13911, V_{62} = 0.13908, V_{63} = 0.13902, V_{64} = 0.12972, V_{65} = 0.12969, V_{66} = 0.12966, V_{67} = 0.13887, V_{68} = 0.13881, V_{69} = 0.13881, V_{70} = 0.14799, V_{71} = 0.12948, V_{72} = 0.12021, V_{73} = 0.12939, V_{74} = 0.11088, V_{75} = 0.12009, V_{76} = 0.12006, V_{77} = 0.09233, V_{78} = 0.10152\big), E\Big)$$

0.6859398543

Turbulent intensity parameter for Martin-Leishman

> $E := \sum_{i=1}^{106} \left(V_i - \xi_i \cdot \left(\frac{1+b}{1+b \cdot \xi_i^{\,4}} \right)^{\frac{1+b}{4 \cdot b}} \right)^2$:

>

> $diff(\%, b)$:

> $DirectSearch$:-$SolveEquations(\%)$

$$\left[5.63321210424161\ 10^{-18}, \left[\ 2.37343887729211\ 10^{-9}\ \right], [b = 1.37685744220585], 25\right]$$

Error n=1 Martin-Leishman

> $E := \sum_{i=1}^{106} \left(V_i - \xi_i \cdot \left(\frac{1 + 1.37685744220585}{1 + 1.37685744220585 \cdot \xi_i^{\,2}} \right)^{\frac{1 + 1.37685744220585}{2 \cdot 1.37685744220585}} \right)^2$:

>

$$subs\Big(\big(V_1 = 0.2939, V_2 = 0.31420, \xi_1 = 0.1287, \xi_2 = 0.1438, V_3 = 0.3446, V_4 = 0.4087, V_5 = 0.4392, V_6 = 0.4966, V_7 = 0.4797, V_8 = 0.5506, V_9 = 0.581, V_{10} = 0.6081, V_{11} = 0.6621, V_{12} = 0.7533, V_{13} = 0.76680, V_{14} = 0.7972, V_{15} = 0.8648, V_{16} = 0.8851, V_{17} = 0.9053, V_{18} = 0.9121, V_{19} = 0.9459, V_{20} = 0.9662, V_{21} = 0.9797, V_{22} = 0.9898, V_{23} = 1.003, V_{24} = 0.9865, V_{25} = 0.9696, V_{26} = 0.9628, V_{27} = 0.9497, V_{28} = 0.9156, V_{29} = 0.8987, V_{30} = 0.8705, V_{31} = 0.8548, V_{32} = 0.8446, V_{33} = 0.8345, V_{34} = 0.8244, V_{35} = 0.8109, V_{36} = 0.7805, V_{37} = 0.7704, V_{38} = 0.7569, V_{39} = 0.7366, V_{40} = 0.7265, V_{41} = 0.713, V_{42} = 0.6927, V_{43} = 0.6826, V_{44} = 0.6657, \xi_3 = 0.159, \xi_4 = 0.2193, \xi_5 = 0.2645, \xi_6 = 0.2647, \xi_7 = 0.2797, \xi_8 = 0.325, \xi_9 = 0.3553, \xi_{10} = 0.3703, \xi_{11} = 0.4306, \xi_{12} = 0.5061, \xi_{13} = 0.5062, \xi_{14} = 0.5514, \xi_{15} = 0.61170, \xi_{16} = 0.64190, \xi_{17} = 0.657, \xi_{18} = 0.672, \xi_{19} = 0.7473, \xi_{20} = 0.7925, \xi_{21} = 0.8377, \xi_{22} = 0.8828, \xi_{23} = 1.003, \xi_{24} = 1.108, \xi_{25} = 1.153, \xi_{26} = 1.214, \xi_{27} = 1.244, \xi_{28} = 1.379, \xi_{29} = 1.454, \xi_{30} = 1.514, \xi_{31} = 1.574, \xi_{32} = 1.589, \xi_{33} = 1.649, \xi_{34} = 1.694, \xi_{35} = 1.739, \xi_{36} = 1.83, \xi_{37} = 1.845, \xi_{38} = 1.905, \xi_{39} = 1.965, \xi_{40} = 2.01, \xi_{41} = 2.085, \xi_{42} = 2.16, \xi_{43} = 2.22, \xi_{44} = 2.28, \xi_{45} = 2.37, \xi_{46} = 2.5, \xi_{47} = 2.551, \xi_{48} = 2.6560, \xi_{49} = 2.7310, \xi_{50} = 2.8360, \xi_{51} = 2.8660, \xi_{52} = 2.942, \xi_{53} = 3.167, \xi_{54} = 3.2120, \xi_{55} = 3.302, \xi_{56} = 3.393, \xi_{57} = 3.438, \xi_{58} = 3.513, \xi_{59} = 3.6030, \xi_{60} = 3.6180, \xi_{61} = 3.663, \xi_{62} = 3.7080, \xi_{63} = 3.768, \xi_{64} = 3.859, \xi_{65} = 3.889, \xi_{66} = 4.084, \xi_{67} = 4.129, \xi_{68} = 4.189, \xi_{69} = 4.25, \xi_{70} = 4.295, \xi_{71} = 4.37, \xi_{72} = 4.505, \xi_{73} = 4.625, \xi_{74} = 4.716, \xi_{75} = 4.806, \xi_{76} = 4.841, \xi_{77} = 4.911, \xi_{78} = 4.956, \xi_{79} = 4.986, \xi_{80} = 5.046, \xi_{81} = 5.167, \xi_{82} = 5.287, \xi_{83} = 5.377, \xi_{84} = 5.4370, \xi_{85} = 5.512, \xi_{86} = 5.618, \xi_{87} = 5.738, \xi_{88} = 5.828, \xi_{89} = 5.873, \xi_{90} = 5.918, \xi_{91} = 5.933, \xi_{92} = 6.204, \xi_{93} = 6.204, \xi_{94} = 6.415, \xi_{95} = 6.49, \xi_{96} = 6.61, \xi_{97} = 6.685, \xi_{98} = 6.73, \xi_{99} = 6.821, \xi_{100} = 6.896, \xi_{101} = 7.136, \xi_{102} = 7.166, \xi_{103} = 7.572, \xi_{104} = 7.723, \xi_{105} = 7.828, \xi_{106} = 7.903, V_{45} = 0.6488, V_{46} = 0.6252, V_{47} = 0.6218, V_{48} = 0.6015, V_{49} = 0.588, V_{50} = 0.5745, V_{51} = 0.5644, V_{52} = 0.5577, V_{53} = 0.5307, V_{54} = 0.5239, V_{55} = 0.5172, V_{56} = 0.507, V_{57} = 0.507, V_{58} = 0.4969, V_{59} = 0.4868, V_{60} = 0.4834, V_{61} = 0.4834, V_{62} = 0.4801, V_{63} = 0.4767, V_{64} = 0.4699, V_{65} = 0.4699, V_{66} = 0.4564, V_{67} = 0.4497, V_{68} = 0.4463, V_{69} = 0.443, V_{70} = 0.443, V_{71} = 0.4362, V_{72} = 0.4295, V_{73} = 0.4227, V_{74} = 0.416, V_{75} = 0.4126, V_{76} = 0.4126, V_{77} = 0.4092, V_{78} = 0.4059, V_{79} = 0.4059, V_{80} = 0.3991, V_{81} = 0.3924, V_{82} = 0.3856, V_{83} = 0.3856, V_{84} = 0.3755, V_{85} = 0.3755, V_{86} = 0.3722, V_{87} = 0.3654, V_{88} = 0.3621, V_{89} = 0.3587, V_{90} = 0.3553, V_{91} = 0.3553, V_{92} = 0.3452, V_{93} = 0.3418, V_{94} = 0.3351, V_{95} = 0.3283, V_{96} = 0.325, V_{97} = 0.3216, V_{98} = 0.3182, V_{99} = 0.3182, V_{100} = 0.3115, V_{101} = 0.3081, V_{102} = 0.3014, V_{103} = 0.2913, V_{104} = 0.2879, V_{105} = 0.2812, V_{106} = 0.2846\big), E\Big)$$

0.7596172117

Error n=2 for Martin Leishman

$$> \quad E := \sum_{i=1}^{106} \left(V_i - \xi_i \cdot \left(\frac{1 + 1.37685744220585}{1 + 1.37685744220585 \cdot \xi_i^{\,4}} \right)^{\frac{1 + 1.37685744220585}{4 \cdot 1.37685744220585}} \right)^2 :$$

>

$$subs\Big(\big(V_1 = 0.2939,\ V_2 = 0.31420,\ \xi_1 = 0.1287,\ \xi_2 = 0.1438,\ V_3 = 0.3446,\ V_4 = 0.4087,\ V_5 = 0.4392,\ V_6 = 0.4966,\ V_7 = 0.4797,\ V_8 = 0.5506,\ V_9 = 0.581,\ V_{10} = 0.6081,\ V_{11} = 0.6621,\ V_{12} = 0.7533,\ V_{13} = 0.76680,\ V_{14} = 0.7972,\ V_{15} = 0.8648,\ V_{16} = 0.8851,\ V_{17} = 0.9053,\ V_{18} = 0.9121,\ V_{19} = 0.9459,\ V_{20} = 0.9662,\ V_{21} = 0.9797,\ V_{22} = 0.9898,\ V_{23} = 1.003,\ V_{24} = 0.9865,\ V_{25} = 0.9696,\ V_{26} = 0.9628,\ V_{27} = 0.9497,\ V_{28} = 0.9156,\ V_{29} = 0.8987,\ V_{30} = 0.8705,\ V_{31} = 0.8548,\ V_{32} = 0.8446,\ V_{33} = 0.8345,\ V_{34} = 0.8244,\ V_{35} = 0.8109,\ V_{36} = 0.7805,\ V_{37} = 0.7704,\ V_{38} = 0.7569,\ V_{39} = 0.7366,\ V_{40} = 0.7265,\ V_{41} = 0.713,\ V_{42} = 0.6927,\ V_{43} = 0.6826,\ V_{44} = 0.6657,\ \xi_3 = 0.159,\ \xi_4 = 0.2193,\ \xi_5 = 0.2645,\ \xi_6 = 0.2647,\ \xi_7 = 0.2797,\ \xi_8 = 0.325,\ \xi_9 = 0.3553,\ \xi_{10} = 0.3703,\ \xi_{11} = 0.4306,\ \xi_{12} = 0.5061,\ \xi_{13} = 0.5062,\ \xi_{14} = 0.5514,\ \xi_{15} = 0.61170,\ \xi_{16} = 0.64190,\ \xi_{17} = 0.657,\ \xi_{18} = 0.672,\ \xi_{19} = 0.7473,\ \xi_{20} = 0.7925,\ \xi_{21} = 0.8377,\ \xi_{22} = 0.8828,\ \xi_{23} = 1.003,\ \xi_{24} = 1.108,\ \xi_{25} = 1.153,\ \xi_{26} = 1.214,\ \xi_{27} = 1.244,\ \xi_{28} = 1.379,\ \xi_{29} = 1.454,\ \xi_{30} = 1.514,\ \xi_{31} = 1.574,\ \xi_{32} = 1.589,\ \xi_{33} = 1.649,\ \xi_{34} = 1.694,\ \xi_{35} = 1.739,\ \xi_{36} = 1.83,\ \xi_{37} = 1.845,\ \xi_{38} = 1.905,\ \xi_{39} = 1.965,\ \xi_{40} = 2.01,\ \xi_{41} = 2.085,\ \xi_{42} = 2.16,\ \xi_{43} = 2.22,\ \xi_{44} = 2.28,\ \xi_{45} = 2.37,\ \xi_{46} = 2.5,\ \xi_{47} = 2.551,\ \xi_{48} = 2.6560,\ \xi_{49} = 2.7310,\ \xi_{50} = 2.8360,\ \xi_{51} = 2.8660,\ \xi_{52} = 2.942,\ \xi_{53} = 3.167,\ \xi_{54} = 3.2120,\ \xi_{55} = 3.302,\ \xi_{56} = 3.393,\ \xi_{57} = 3.438,\ \xi_{58} = 3.513,\ \xi_{59} = 3.6030,\ \xi_{60} = 3.6180,\ \xi_{61} = 3.663,\ \xi_{62} = 3.7080,\ \xi_{63} = 3.768,\ \xi_{64} = 3.859,\ \xi_{65} = 3.889,\ \xi_{66} = 4.084,\ \xi_{67} = 4.129,\ \xi_{68} = 4.189,\ \xi_{69} = 4.25,\ \xi_{70} = 4.295,\ \xi_{71} = 4.37,\ \xi_{72} = 4.505,\ \xi_{73} = 4.625,\ \xi_{74} = 4.716,\ \xi_{75} = 4.806,\ \xi_{76} = 4.841,\ \xi_{77} = 4.911,\ \xi_{78} = 4.956,\ \xi_{79} = 4.986,\ \xi_{80} = 5.046,\ \xi_{81} = 5.167,\ \xi_{82} = 5.287,\ \xi_{83} = 5.377,\ \xi_{84} = 5.4370,\ \xi_{85} = 5.512,\ \xi_{86} = 5.618,\ \xi_{87} = 5.738,\ \xi_{88} = 5.828,\ \xi_{89} = 5.873,\ \xi_{90} = 5.918,\ \xi_{91} = 5.933,\ \xi_{92} = 6.204,\ \xi_{93} = 6.204,\ \xi_{94} = 6.415,\ \xi_{95} = 6.49,\ \xi_{96} = 6.61,\ \xi_{97} = 6.685,\ \xi_{98} = 6.73,\ \xi_{99} = 6.821,\ \xi_{100} = 6.896,\ \xi_{101} = 7.136,\ \xi_{102} = 7.166,\ \xi_{103} = 7.572,\ \xi_{104} = 7.723,\ \xi_{105} = 7.828,\ \xi_{106} = 7.903,\ V_{45} = 0.6488,\ V_{46} = 0.6252,\ V_{47} = 0.6218,\ V_{48} = 0.6015,\ V_{49} = 0.588,\ V_{50} = 0.5745,\ V_{51} = 0.5644,\ V_{52} = 0.5577,\ V_{53} = 0.5307,\ V_{54} = 0.5239,\ V_{55} = 0.5172,\ V_{56} = 0.507,\ V_{57} = 0.507,\ V_{58} = 0.4969,\ V_{59} = 0.4868,\ V_{60} = 0.4834,\ V_{61} = 0.4834,\ V_{62} = 0.4801,\ V_{63} = 0.4767,\ V_{64} = 0.4699,\ V_{65} = 0.4699,\ V_{66} = 0.4564,\ V_{67} = 0.4497,\ V_{68} = 0.4463,\ V_{69} = 0.443,\ V_{70} = 0.443,\ V_{71} = 0.4362,\ V_{72} = 0.4295,\ V_{73} = 0.4227,\ V_{74} = 0.416,\ V_{75} = 0.4126,\ V_{76} = 0.4126,\ V_{77} = 0.4092,\ V_{78} = 0.4059,\ V_{79} = 0.4059,\ V_{80} = 0.3991,\ V_{81} = 0.3924,\ V_{82} = 0.3856,\ V_{83} = 0.3856,\ V_{84} = 0.3755,\ V_{85} = 0.3755,\ V_{86} = 0.3722,\ V_{87} = 0.3654,\ V_{88} = 0.3621,\ V_{89} = 0.3587,\ V_{90} = 0.3553,\ V_{91} = 0.3553,\ V_{92} = 0.3452,\ V_{93} = 0.3418,\ V_{94} = 0.3351,\ V_{95} = 0.3283,\ V_{96} = 0.325,\ V_{97} = 0.3216,\ V_{98} = 0.3182,\ V_{99} = 0.3182,\ V_{100} = 0.3115,\ V_{101} = 0.3081,\ V_{102} = 0.3014,\ V_{103} = 0.2913,\ V_{104} = 0.2879,\ V_{105} = 0.2812,\ V_{106} = 0.2846\big),\ E\Big)$$

0.1087506138

Error n=3 Martin-Leishman

$$E := \sum_{i=1}^{106} \left(V_i - \xi_i \cdot \left(\frac{1 + 1.37685744220585}{1 + 1.37685744220585 \cdot \xi_i^{\,6}} \right)^{\frac{1 + 1.37685744220585}{6 \cdot 1.37685744220585}} \right)^2 :$$

>

$$subs\Big(\big(V_1 = 0.2939, V_2 = 0.31420, \xi_1 = 0.1287, \xi_2 = 0.1438, V_3 = 0.3446, V_4 = 0.4087, V_5 = 0.4392, V_6 = 0.4966, V_7 = 0.4797, V_8 = 0.5506, V_9 = 0.581, V_{10} = 0.6081, V_{11} = 0.6621, V_{12} = 0.7533, V_{13} = 0.76680, V_{14} = 0.7972, V_{15} = 0.8648, V_{16} = 0.8851, V_{17} = 0.9053, V_{18} = 0.9121, V_{19} = 0.9459, V_{20} = 0.9662, V_{21} = 0.9797, V_{22} = 0.9898, V_{23} = 1.003, V_{24} = 0.9865, V_{25} = 0.9696, V_{26} = 0.9628, V_{27} = 0.9497, V_{28} = 0.9156, V_{29} = 0.8987, V_{30} = 0.8705, V_{31} = 0.8548, V_{32} = 0.8446, V_{33} = 0.8345, V_{34} = 0.8244, V_{35} = 0.8109, V_{36} = 0.7805, V_{37} = 0.7704, V_{38} = 0.7569, V_{39} = 0.7366, V_{40} = 0.7265, V_{41} = 0.713, V_{42} = 0.6927, V_{43} = 0.6826, V_{44} = 0.6657, \xi_3 = 0.159, \xi_4 = 0.2193, \xi_5 = 0.2645, \xi_6 = 0.2647, \xi_7 = 0.2797, \xi_8 = 0.325, \xi_9 = 0.3553, \xi_{10} = 0.3703, \xi_{11} = 0.4306, \xi_{12} = 0.5061, \xi_{13} = 0.5062, \xi_{14} = 0.5514, \xi_{15} = 0.61170, \xi_{16} = 0.64190, \xi_{17} = 0.657, \xi_{18} = 0.672, \xi_{19} = 0.7473, \xi_{20} = 0.7925, \xi_{21} = 0.8377, \xi_{22} = 0.8828, \xi_{23} = 1.003, \xi_{24} = 1.108, \xi_{25} = 1.153, \xi_{26} = 1.214, \xi_{27} = 1.244, \xi_{28} = 1.379, \xi_{29} = 1.454, \xi_{30} = 1.514, \xi_{31} = 1.574, \xi_{32} = 1.589, \xi_{33} = 1.649, \xi_{34} = 1.694, \xi_{35} = 1.739, \xi_{36} = 1.83, \xi_{37} = 1.845, \xi_{38} = 1.905, \xi_{39} = 1.965, \xi_{40} = 2.01, \xi_{41} = 2.085, \xi_{42} = 2.16, \xi_{43} = 2.22, \xi_{44} = 2.28, \xi_{45} = 2.37, \xi_{46} = 2.5, \xi_{47} = 2.551, \xi_{48} = 2.6560, \xi_{49} = 2.7310, \xi_{50} = 2.8360, \xi_{51} = 2.8660, \xi_{52} = 2.942, \xi_{53} = 3.167, \xi_{54} = 3.2120, \xi_{55} = 3.302, \xi_{56} = 3.393, \xi_{57} = 3.438, \xi_{58} = 3.513, \xi_{59} = 3.6030, \xi_{60} = 3.6180, \xi_{61} = 3.663, \xi_{62} = 3.7080, \xi_{63} = 3.768, \xi_{64} = 3.859, \xi_{65} = 3.889, \xi_{66} = 4.084, \xi_{67} = 4.129, \xi_{68} = 4.189, \xi_{69} = 4.25, \xi_{70} = 4.295, \xi_{71} = 4.37, \xi_{72} = 4.505, \xi_{73} = 4.625, \xi_{74} = 4.716, \xi_{75} = 4.806, \xi_{76} = 4.841, \xi_{77} = 4.911, \xi_{78} = 4.956, \xi_{79} = 4.986, \xi_{80} = 5.046, \xi_{81} = 5.167, \xi_{82} = 5.287, \xi_{83} = 5.377, \xi_{84} = 5.4370, \xi_{85} = 5.512, \xi_{86} = 5.618, \xi_{87} = 5.738, \xi_{88} = 5.828, \xi_{89} = 5.873, \xi_{90} = 5.918, \xi_{91} = 5.933, \xi_{92} = 6.204, \xi_{93} = 6.204, \xi_{94} = 6.415, \xi_{95} = 6.49, \xi_{96} = 6.61, \xi_{97} = 6.685, \xi_{98} = 6.73, \xi_{99} = 6.821, \xi_{100} = 6.896, \xi_{101} = 7.136, \xi_{102} = 7.166, \xi_{103} = 7.572, \xi_{104} = 7.723, \xi_{105} = 7.828, \xi_{106} = 7.903, V_{45} = 0.6488, V_{46} = 0.6252, V_{47} = 0.6218, V_{48} = 0.6015, V_{49} = 0.588, V_{50} = 0.5745, V_{51} = 0.5644, V_{52} = 0.5577, V_{53} = 0.5307, V_{54} = 0.5239, V_{55} = 0.5172, V_{56} = 0.507, V_{57} = 0.507, V_{58} = 0.4969, V_{59} = 0.4868, V_{60} = 0.4834, V_{61} = 0.4834, V_{62} = 0.4801, V_{63} = 0.4767, V_{64} = 0.4699, V_{65} = 0.4699, V_{66} = 0.4564, V_{67} = 0.4497, V_{68} = 0.4463, V_{69} = 0.443, V_{70} = 0.443, V_{71} = 0.4362, V_{72} = 0.4295, V_{73} = 0.4227, V_{74} = 0.416, V_{75} = 0.4126, V_{76} = 0.4126, V_{77} = 0.4092, V_{78} = 0.4059, V_{79} = 0.4059, V_{80} = 0.3991, V_{81} = 0.3924, V_{82} = 0.3856, V_{83} = 0.3856, V_{84} = 0.3755, V_{85} = 0.3755, V_{86} = 0.3722, V_{87} = 0.3654, V_{88} = 0.3621, V_{89} = 0.3587, V_{90} = 0.3553, V_{91} = 0.3553, V_{92} = 0.3452, V_{93} = 0.3418, V_{94} = 0.3351, V_{95} = 0.3283, V_{96} = 0.325, V_{97} = 0.3216, V_{98} = 0.3182, V_{99} = 0.3182, V_{100} = 0.3115, V_{101} = 0.3081, V_{102} = 0.3014, V_{103} = 0.2913, V_{104} = 0.2879, V_{105} = 0.2812, V_{106} = 0.2846\big), E\Big)$$

0.3243911345

Appendix B

Similarity

$\xi = r / r_c$ and $\tau = 1 + 4\dfrac{\nu t}{r_c^2}$, $\tau = 1 + 4\tau'$, $\tau' = \dfrac{\nu t}{r_c^2}$

Let

$\eta = \xi / \sqrt{\tau}$ $\rightarrow$ $\xi = \eta\sqrt{\tau}$ and $V(\tau, \xi)\sqrt{\tau} = g(\eta)$

θ-momentum

$$\frac{\partial V}{\partial \tau'} + u(\tau', \xi)\left(\frac{\partial V}{\partial \xi} + \frac{V}{\xi}\right) = \left\{\frac{\partial^2 V}{\partial \xi^2} + \frac{1}{\xi}\frac{\partial V}{\partial \xi} - \frac{V}{\xi^2}\right\}$$

$$\frac{\partial V}{\partial \tau'} = \frac{\partial V}{\partial \tau}\frac{\partial \tau}{\partial \tau'} = \frac{\partial V}{\partial \tau}\frac{\partial(1 + 4\,\tau')}{\partial \tau'} = 4\frac{\partial V}{\partial \tau}$$

$$4\frac{\partial V}{\partial \tau} + u(\tau, \xi)\left(\frac{\partial V}{\partial \xi} + \frac{V}{\xi}\right) = \left\{\frac{\partial^2 V}{\partial \xi^2} + \frac{1}{\xi}\frac{\partial V}{\partial \xi} - \frac{V}{\xi^2}\right\}$$

(i) (ii) (iii) (iv) (v)

Term (i)

$$4\frac{\partial V}{\partial \tau}=\frac{\partial}{\partial \tau}\left(\frac{g(\eta)}{\sqrt{\tau}}\right)=4\left\{-\frac{1}{2\,\tau^{3/2}}\,g(\eta)\;+\frac{1}{\sqrt{\tau}}\,g'(\eta)\,\frac{\partial \eta}{\partial \tau}\right\}\qquad g'\equiv\frac{d\,g}{\partial \eta}$$

$$\frac{\partial \eta}{\partial \tau}-\frac{1}{2}\,\frac{\xi}{\tau^{3/2}}$$

$$4\frac{\partial V}{\partial \tau}=\frac{\partial}{\partial \tau}\left(\frac{g(\eta)}{\sqrt{\tau}}\right)+4\left\{-\frac{1}{2\tau^{3/2}}g(\eta)-\frac{1}{2}\frac{1}{\tau^{3/2}}\frac{\xi}{\sqrt{\tau}}g'(\eta)\right\}=-\frac{2}{\tau^{3/2}}\left(g(\eta)+\frac{\xi}{\sqrt{\tau}}g'(\eta)\right)$$

$$4\,\frac{\partial V}{\partial \tau}=\;-\frac{2}{\tau^{3/2}}\left(g\,(\eta)+\eta\,g'(\eta)\right)=-\frac{2}{\tau^{3/2}}\,\frac{d}{d\eta}\left(\eta\,g(\eta)\,\right)\qquad\text{(i)}$$

Term (iv)

$$\frac{\partial V}{\partial \xi}=\frac{\partial}{\partial \eta}\left(\frac{g(\eta)}{\sqrt{\tau}}\right)\frac{\partial \eta}{\partial \xi}=\frac{1}{\sqrt{\tau}}\,g'\,(\eta)\frac{\partial \eta}{\partial \xi}=\frac{1}{\tau}\,g'\,(\eta)\frac{\partial \eta}{\partial \xi}$$

$$\frac{\partial V}{\partial \xi}=\frac{\partial}{\partial \eta}\left(\frac{g\,(\eta)}{\sqrt{\tau}}\right)\frac{\partial \eta}{\partial \xi}=\frac{1}{\sqrt{\tau}}\,g'(\eta)\,\frac{\partial \eta}{\partial \xi}=\frac{1}{\tau}\,g'(\eta)\qquad\frac{\partial \eta}{\partial R}=\frac{1}{\sqrt{\tau}}$$

$$\frac{1}{\xi}\,\frac{\partial V}{\partial \xi}=\frac{\partial}{\partial \eta}\left(\frac{g(\eta)}{\sqrt{\tau}}\right)\frac{\partial \eta}{\partial \xi}=\frac{1}{\sqrt{\tau}}\,g'(\eta)\,\frac{\partial \eta}{\partial \xi}=\frac{1}{\tau\,\xi}\,g'(\eta)$$

$$\frac{1}{\xi}\frac{\partial V}{\partial \xi}=\frac{\partial}{\partial \eta}\left(\frac{g(\eta)}{\sqrt{\tau}}\right)\frac{\partial \eta}{\partial \xi}=\frac{1}{\sqrt{\tau}}g'(\eta)\frac{\partial \eta}{\partial \xi}=\frac{1}{\tau\,\xi}g'(\eta) \qquad \text{(iv)}$$

Term (iii)

$$\frac{\partial^2 V}{\partial \xi^2}=\frac{\partial}{\partial \xi}\frac{\partial V}{\partial \xi}=\frac{\partial}{\partial \eta}\left(\frac{1}{\tau}g'(\eta)\right)\frac{\partial \eta}{\partial \xi}=\frac{1}{\tau^{3/2}}g''(\eta)$$

$$\frac{\partial^2 V}{\partial \xi^2}=\frac{\partial}{\partial \xi}\frac{\partial V}{\partial \xi}=\frac{\partial}{\partial \eta}\left(\frac{1}{\tau}g'(\eta)\right)\frac{\partial \eta}{\partial \xi}=\frac{1}{\tau^{3/2}}g''(\eta) \qquad \text{(iii)}$$

Term (v)

$$\frac{V(\tau,\xi)}{\xi^2}=\frac{g(\eta)}{\sqrt{\tau}\,\xi^2}$$

$$\frac{V(\tau,\xi)}{\xi^2}=\frac{g(\eta)}{\sqrt{\tau}\,\xi^2} \qquad \text{(v)}$$

Term (ii)

$$\frac{V(\tau,R)}{\xi}=\frac{g(\eta)}{\sqrt{\tau}\,\xi}$$

$$\frac{\partial V}{\partial R} = \frac{1}{\tau} g'(\eta)$$

$$u(\tau, \xi)\left(\frac{\partial V}{\partial \xi} + \frac{V}{\xi}\right) = u(\tau, \xi)\left(\frac{1}{\tau} g'(\eta) + \frac{g(\eta)}{\sqrt{\tau}\ \xi}\right)$$

$$u(\tau, \xi)\left(\frac{\partial V}{\partial \xi} + \frac{V}{\xi}\right) = u(\tau, \xi)\left(\frac{1}{\tau} g'(\eta) + \frac{g(\eta)}{\sqrt{\tau}\ \xi}\right) \quad \text{(ii)}$$

$$\frac{\partial V}{\partial \tau} = -\frac{1}{2\ \tau^{3/2}} \frac{d}{d\eta}\left(\eta\, g(\eta)\right) \quad \text{(i)}$$

$$u(\tau, \xi)\left(\frac{\partial V}{\partial \xi} + \frac{V}{\xi}\right) = u(\tau, \xi)\left(\frac{1}{\tau} g'(\eta) + \frac{g(\eta)}{\sqrt{\tau}\ \xi}\right) \quad \text{(ii)}$$

$$\frac{\partial^2 V}{\partial \xi^2} = \frac{1}{\tau^{3/2}} g''(\eta) \quad \text{(iii)}$$

$$\frac{1}{\xi} \frac{\partial V}{\partial \xi} = \frac{1}{\tau\ \xi} g'(\eta) \quad \text{(iv)}$$

$$\frac{V}{\xi^2} = \frac{g(\eta)}{\sqrt{\tau}\ \xi} \quad \text{(v)}$$

From the tangential momentum we have:

$$-\frac{2}{\tau^{3/2}}\frac{d}{d\eta}\left(\eta\, g(\eta)\right)+u(\tau,\xi)\left(\frac{1}{\tau}g'(\eta)+\frac{g(\eta)}{\sqrt{\tau}\,\xi}\right)=\left\{\frac{1}{\tau^{3/2}}g''(\eta)+\frac{1}{\tau\,\xi}g'(\eta)-\frac{g(\eta)}{\sqrt{\tau}\,\xi^2}\right\}$$

$$-\frac{2}{\tau^{3/2}}\frac{d}{d\eta}\left(\eta\, g(\eta)\right)+u(\tau,\xi)\left(\frac{1}{\tau}g'(\eta)+\frac{g(\eta)}{\sqrt{\tau}\,\xi}\right)=\frac{1}{\tau^{3/2}}\left[g''(\eta)+\frac{\sqrt{\tau}}{\xi}g'(\eta)-\frac{g(\eta)\,\tau}{\xi^2}\right]$$

$$-\frac{2}{\tau^{3/2}}\frac{d}{d\eta}\left(\eta\, g(\eta)\right)+u(\tau,\xi)\left(\frac{1}{\tau}g'(\eta)+\frac{g(\eta)}{\tau\,\eta}\right)=\frac{1}{\tau^{3/2}}\left[g''(\eta)+\frac{1}{\frac{\xi}{\sqrt{\tau}}}g'(\eta)-\frac{g(\eta)}{\frac{\xi^2}{\tau}}\right]$$

$$-\frac{2}{\tau^{3/2}}\frac{d}{d\eta}\left(\eta\, g(\eta)\right)+\frac{u(\tau,\xi)}{\tau}\left(g'(\eta)+\frac{g(\eta)}{\eta}\right)=\frac{1}{\tau^{3/2}}\left[g''(\eta)+\frac{1}{\frac{\xi}{\sqrt{\tau}}}g'(\eta)-\frac{g(\eta)}{\frac{\xi^2}{\tau}}\right]$$

$$-2\frac{d}{d\eta}\left(\eta\, g(\eta)\right)+u(\tau,\xi)\sqrt{\tau}\left(g'(\eta)+\frac{g(\eta)}{\eta}\right)=\left\{g''(\eta)+\frac{1}{\eta}g'(\eta)-\frac{g(\eta)}{\eta^2}\right\}$$

$$-2\,\eta\frac{1}{\eta}\frac{d}{d\eta}\left(\eta\, g(\eta)\right)+u(\tau,\xi)\sqrt{\tau}\,\frac{1}{\eta}\frac{d}{d\eta}\left(\eta g(\eta)\right)=\left\{g''(\eta)+\frac{1}{\eta}g'(\eta)-\frac{g(\eta)}{\eta^2}\right\}$$

$$\left\{u(\tau,R)\sqrt{\tau}-2\eta\right\}\frac{1}{\eta}\frac{d}{d\eta}\left(\eta g(\eta)\right)=g''(\eta)+\frac{1}{\eta}g'(\eta)-\frac{g(\eta)}{\eta^2}$$

If we take $U(\eta)=u(\tau,\xi)\sqrt{\tau}-2\eta$ then we obtain:

$$\frac{U(\eta)}{\eta}\frac{d}{d\eta}\left(\eta g(\eta)\right)=\frac{d}{d\eta}\left(\frac{1}{\eta}\frac{d}{d}\left(\eta\, g(\eta)\right)\right) \qquad \text{(a)}$$

Continuity:

$$\frac{\partial}{\partial R}u(\tau,\xi)+\frac{u(\tau,\xi)}{\xi}+h(\tau,\xi)=0$$

$$\frac{1}{\sqrt{\tau}}\frac{\partial}{\partial R}u(\tau,\xi)\sqrt{\tau}+\frac{u(\tau,\xi)}{\xi}+h(\tau,\xi)=0$$

$$\frac{1}{\sqrt{\tau}}\frac{\partial}{\partial \xi}U(\eta)+\frac{u(\tau,\xi)}{\xi}+h(\tau,\xi)=0$$

$$\frac{1}{\sqrt{\tau}}\frac{dU(\eta)}{d\eta}\frac{\partial U(\eta)}{\partial \xi}+\frac{u(\tau,\xi)}{\xi}+h(\tau,\xi)=0$$

$$\frac{1}{\tau}\frac{dU(\eta)}{d\eta}+\frac{u(\tau,\xi)}{\xi}+h(\tau,\xi)=0$$

$$\frac{dU(\eta)}{d\eta}+\frac{U(\eta)}{\eta}+h(\tau,\xi)\,\tau=0$$

$$\frac{1}{\eta}\frac{d}{d\eta}\left[\eta\, U(\eta)\right]+h(\tau,\,\xi)\;\tau=0$$

Continuity

$$\frac{1}{\eta}\frac{d}{d\eta}\left[\eta\, U(\eta)\right]+H(\eta)=0 \qquad \text{where} \qquad H(\eta)=h(\tau,\,R)\;\tau \tag{b}$$

$$H(\eta)=-\frac{1}{\eta}\frac{d}{d\eta}\left[\eta\, U(\eta)\right]$$

r-momentum

$$\frac{\left[V(\tau,\,\xi)\,\right]^2}{\xi}=\frac{\partial\Delta p(\tau,\,\xi)}{\partial\xi}$$

$$\frac{\left[V(\tau,\,\xi)\sqrt{\tau}\,\right]^2}{\tau\xi}=\frac{\partial\Delta p(\tau,\,\xi)}{\partial\xi}$$

$$\frac{\left[V(\tau,\,\xi)\sqrt{\tau}\,\right]^2}{\tau\sqrt{\tau}\;\eta}=\frac{\partial\Delta p(\tau,\,\xi)}{\partial\xi}$$

$$\frac{\left[V(\tau,\xi)\sqrt{\tau}\right]^2}{\sqrt{\tau}\ \eta} = \frac{\partial}{\partial\xi}\left(\tau\ \Delta p(\tau,\xi)\right) = \frac{d}{d\eta}\left(\Delta\Pi(\eta)\right)\frac{\partial\eta}{\partial\xi} = \frac{d}{d\eta}\left(\Delta\Pi(\eta)\right)\frac{1}{\sqrt{\tau}}$$

where $\Delta\Pi(\eta) = p\,(\tau,\xi)\ \tau$

r-momentum

$$\frac{\left[g(\eta)\right]^2}{\eta} = \frac{d}{d\eta}\left(\Delta\Pi(\eta)\right) \qquad \text{(c)}$$

Equations (a), (b), and (c) are analogous to those that have produced several steady solutions.